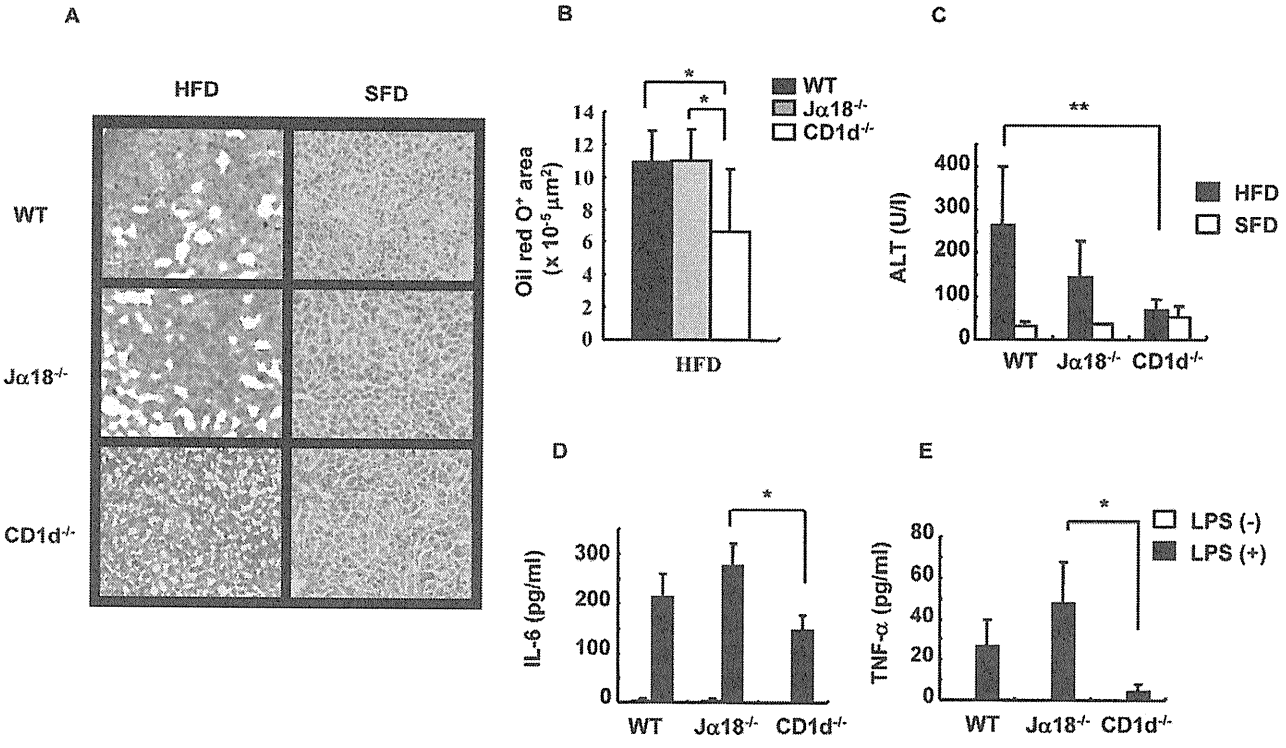

Figure 3. Histology and cytokine production in the liver. (A) A liver section was stained with ORO (frozen section) in SFD- and HFD-fed mice. (B) Red-stained lipid droplets in liver sections of HFD-fed mice were quantified with image analysis software. (C) Serum levels of ALT were quantified with the Drychem system. (D, E) The production of cytokines from HMNC of HFD-fed mice stimulated with LPS for 20 h (n = 3–4 female mice in each group). The results are expressed as mean ± s.d. Statistical analysis was performed according to the Tukey-Kramer test. *$p<0.05$, **$p<0.01$.
doi:10.1371/journal.pone.0030568.g003

each adipocyte was morphometrically compared (Figure 4B). The adipocytes from CD1d$^{-/-}$ mice had significantly smaller circumference than those from WT and Jα18$^{-/-}$ mice.

When leptin is overexpressed, mice demonstrate a lean phenotype [23]. To examine whether CD1d$^{-/-}$ expressed a higher level of leptin in sera than WT and Jα18$^{-/-}$ mice, serum leptin levels were quantified. However, CD1d$^{-/-}$ showed the lowest level among the three strains of mice, which was proportional to the volume of WAT (Figure 4C).

Analysis of infiltrated cellular components in liver of mice fed an HFD

Our findings thus far showed that adiposity and hepatosteatosis were similar between WT and Jα18$^{-/-}$ but were minimal in CD1d$^{-/-}$ mice. The difference between Jα18$^{-/-}$ and CD1d$^{-/-}$ mice is solely the absence of type II NKT cells selected by CD1d in CD1d$^{-/-}$ but not Jα18$^{-/-}$ mice. To study the relationship between type I (iNKT) and type II NKT cells, we analyzed NKT cell subsets in liver and adipose tissue of each strain. As shown in our previous report with the short term feeding of HFD [18], the proportion of NKT cells in liver decreased in WT mice fed an HFD compared to mice on an SFD when the HMNC fraction was stained with a combination of either α-GalCer-loaded CD1d-dimer and anti-TCRβ mAb (iNKT cells) (Figure 5A-a, b; 22.8%−>6.8%) or anti-NK1.1 and TCRβ mAb (total NKT cells, including NKT-like cells) (Figure 5A-c, d; 27.9%−>6.6%). To detect the subset of type II NKT cells and NKT-like cells in the iNKT cell-deficient strains, the latter combination was employed. Although a significant decrease was demonstrated in NKT cells in WT mice (Figure 5B-a), there was no significant difference in the proportion of total NKT cells in Jα18$^{-/-}$ and CD1d$^{-/-}$ mice fed an HFD (Figure 5B-a), but Jα18$^{-/-}$ mice appeared to exhibit a slight decrease in the prevalence of these cells on an HFD. To examine the residual NKT-like cells in the livers of Jα18$^{-/-}$ and CD1d$^{-/-}$ mice, staining with a combination of anti-NK1.1 and anti-TCRβ mAb was employed. As demonstrated in the FACS profiles, total NKT cells in WT mice were significantly decreased after HFD feeding (Figure 5B-a). As for the subset of residual NKT cells, the subset that expressed neither CD4 nor CD8 (CD4$^-$8$^-$ double negative; DN) did not differ regardless of the feeding regimen used or the mouse strains analyzed. The relative prevalence of the CD4$^+$8$^-$ subset was as follows: WT>Jα18$^{-/-}$>CD1d$^{-/-}$ mice, and the prevalence of the CD4$^-$8$^+$ subset had an inverse relationship with CD8$^+$ cells (WT<Jα18$^{-/-}$<CD1d$^{-/-}$ mice) (Figure 5B-b, c). Although the total number of liver NKT cells was reduced, the residual population was mainly a CD4$^+$ subset in WT mice and the remaining cells were a CD4$^-$8$^-$ subset (Figure 5B-d). The CD8$^+$ subset was very minimal in WT mice. On the other hand, CD1d$^{-/-}$ mice had residual numbers of hepatic NK1.1$^+$TCRβ$^+$, NKT-like cells, and about 40~50% of the population was CD8$^+$. There was no significant difference in the proportion of regulatory T (T_{reg}) cells in HMNC among the three strains of mice (data not shown). It should be noted that NKT cells in the liver of WT mice fed with HFD were significantly reduced. This effect of lipid excess was evident as early as day 1 of HFD feeding (data not shown).

Analysis of infiltrated cellular components in adipose tissue of mice fed an HFD

The SVF in adipose tissue contains innate lymphocytes and Mϕ even under normal conditions. In adipose tissue in obese mice, we

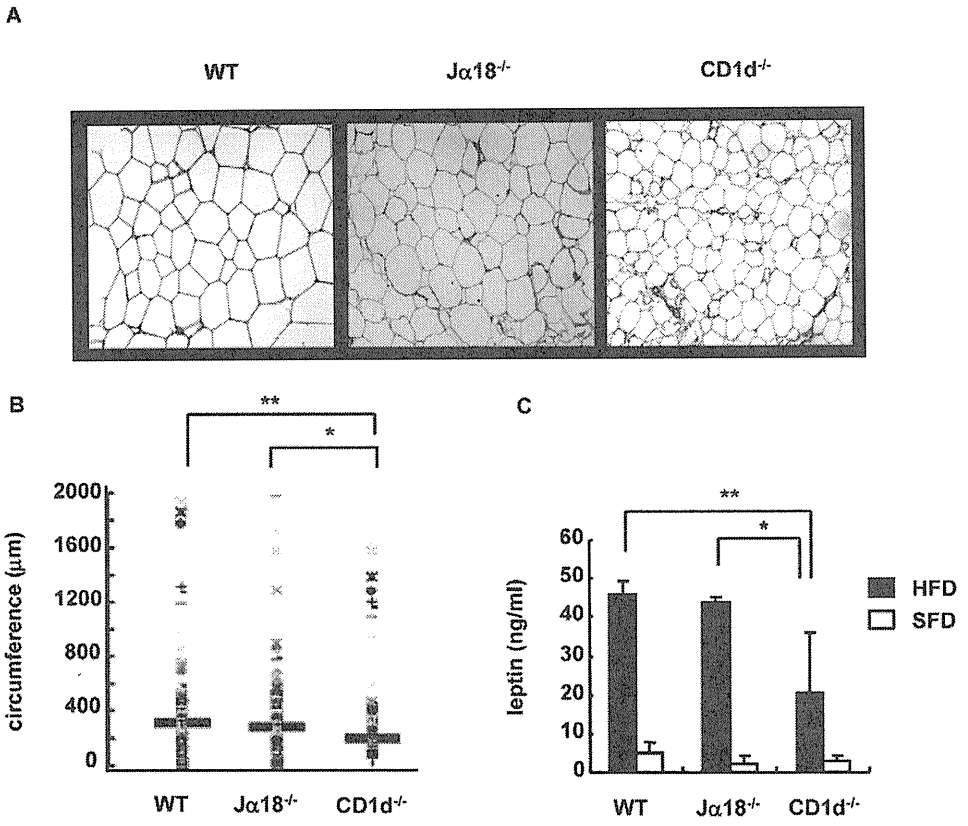

Figure 4. Histology of perigonadal adipose tissue and serum leptin level. (A, B) A paraffin section of perigonadal adipose tissue was stained with HE, and the circumference of adipocytes was morphometrically analyzed (10×10, 300–400 adipocytes measured) in HFD mice. (C) The serum leptin level was quantified by ELISA (n = 3–4 female mice in each group). Representative data of two similar experiments are shown. The results are expressed as mean ± s.d. Statistical analysis was performed according to the Tukey-Kramer test. *$p<0.05$, **$p<0.01$.
doi:10.1371/journal.pone.0030568.g004

readily detected increased numbers of mononuclear cells than in lean mice in spaces surrounded by adipocytes (data not shown). First, we analyzed NK1.1$^+$TCRβ$^+$ (NKT) cells and the CD4/8 subsets. Since the CD1d-restricted NKT cells are absent in CD1d$^{-/-}$ mice, we used NK1.1$^+$TCRβ$^+$ staining to detect residual NKT-like cells instead of double stainig with a combination of α-GalCer-loaded CD1d-dimers and anti-TCRβ mAb. In WT mice, the proportion of iNKT cells in adipose tissue was not significantly different (Figure 6A-a, b; 1.5%−>1.2%), whereas there were significantly more NK1.1$^+$TCRβ$^+$ cells in mice fed an HFD compared to those on SFD, in the same experimental setting (Figure 6A-c, d; 2.2%−>5.2%). The percentage of NKT cells increased in WT and Jα18$^{-/-}$ cells when the NKT cells of mice on HFD were compared with those on SFD (WT; $p<0.05$; Jα18$^{-/-}$; $p<0.01$), whereas such an increase was not observed in CD1d$^{-/-}$ mice (Figure 6B-a). Since CD1d$^{-/-}$ mice lack CD4$^+$ CD1d-restricted NKT cells, there were significant differences in the percentages (Figure 6B-b) (WT; $p<0.05$; Jα18$^{-/-}$; $p<0.01$) and actual cell numbers (WT, Jα18$^{-/-}$; $p<0.05$). Of note, the CD8$^+$ subset was prominently increased in the adipose tissue of Jα18$^{-/-}$ mice both in percentage (Figure 6B-c) and in number. The CD4$^-$8$^-$ subset of NKT cells appeared to be significantly decreased in Jα18$^{-/-}$ mice fed an HFD, most likely due to the relative abundance of the CD4$^-$8$^+$ subset (Figure 6B-d). Similar results were obtained when analyzing actual cell numbers (WT>Jα18$^{-/-}$>CD1d$^{-/-}$) (data not shown).

We analyzed and compared the proportion of NKT cells at early and late phases (18-wk) of HFD feeding. In WT mice, the number of α-GalCer-CD1d-dimer$^+$ cells and NK1.1$^+$TCRβ$^+$ cells in liver were increased at 1 wk of HFD-feeding, and numbers tended to decrease thereafter (Figure S3A). On the other hand, these cells, especially the NK1.1$^+$TCRβ$^+$ population, were gradually increased in adipose tissue (Figure S3B). The increase in NK1.1$^+$TCRβ$^+$ cells (percentage in SVF) in adipose tissue correlated with BW in WT and Jα18$^{-/-}$ mice, whereas no correlation was found in CD1d$^{-/-}$ mice (Figure 6C). A similar correlation was obtained between numbers of NK1.1$^+$TCRβ$^+$ cells (cell number/g adipose tissue) and BW (data not shown).

Analysis of Mφ in adipose tissue and cytokine production upon LPS stimulation

Mφ are another major cellular subset in SVF and may affect the metabolism of adipose tissue. Therefore, SVF preparations from the three strains of mouse were stained with F4/80 and CD11b (Figure 7A). The three strains had a similar pattern of F4/80$^+$/CD11b$^+$ staining. Although we anticipated that CD1d$^{-/-}$ mice had fewer Mφ than Jα18$^{-/-}$ mice, the percentage of F4/80$^+$/CD11b$^+$ cells in CD1d$^{-/-}$ mice was higher than that of Jα18$^{-/-}$ mice (Figure 7B-a). However, when the F4/80$^+$ population was divided into two subpopulations according to the MFI of F4/80 staining pattern, i. e., Population 1 (P1: F4/80^{high}) and Population 2 (P2: F4/80$^{low\sim-}$) cells (both CD11b$^+$), WT mice had higher frequencies of P1 than Jα18$^{-/-}$ mice (Figure 7B-b), whereas CD1d$^{-/-}$ mice had an increased frequency of P2 than WT and Jα18$^{-/-}$ mice (Figure 7B-c). Analyses of actual cell numbers

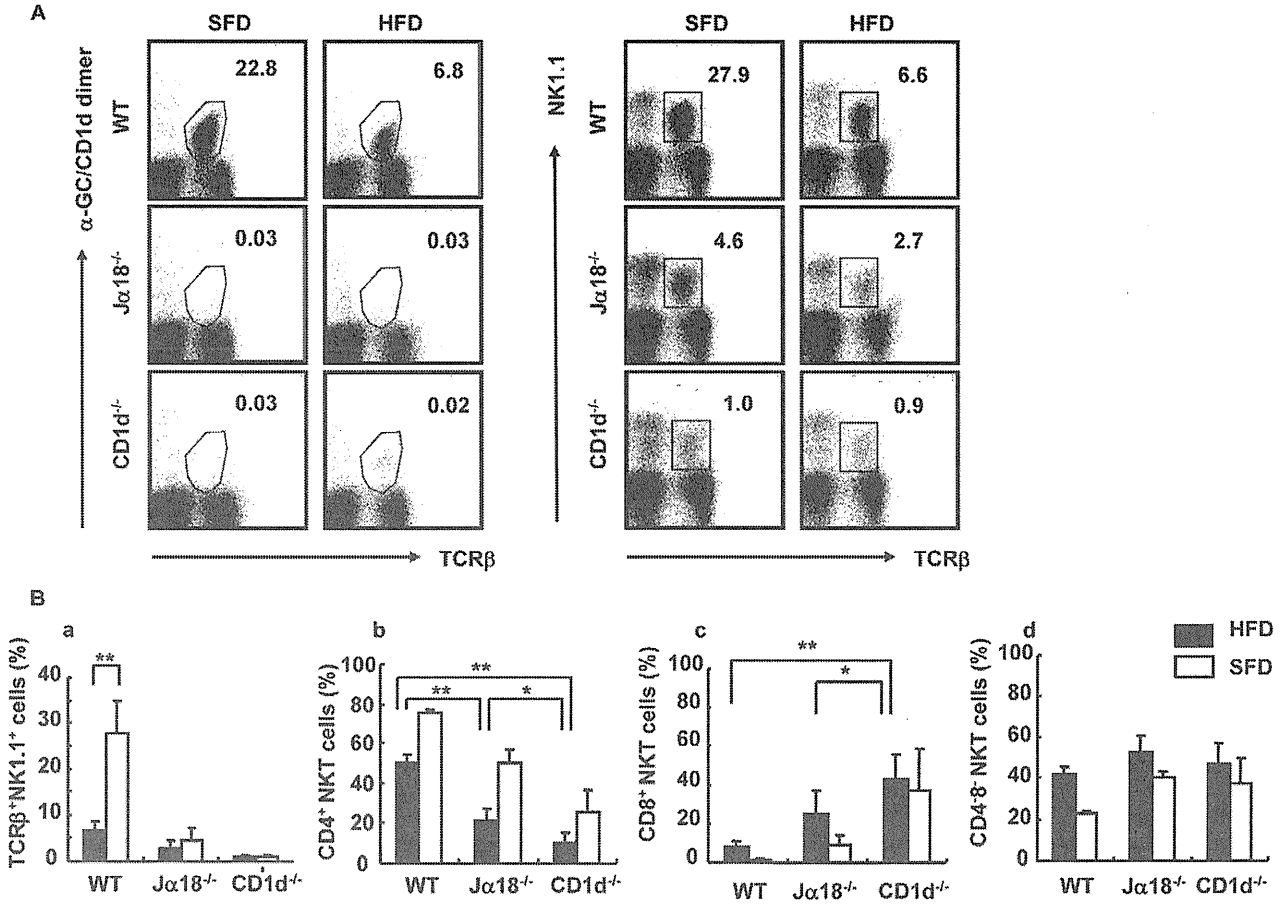

Figure 5. Flow cytometric analyses of HMNC in mice fed an SFD or an HFD. (A) A representative flow cytometric dot-plot defining the population of α-GalCer/CD1d dimer$^+$TCRβ$^+$ and NK1.1$^+$TCRβ$^+$ cells in the liver of SFD-fed mice (a, c) and HFD-fed mice (b, d). (B) The proportion of NK1.1$^+$TCRβ$^+$ cells (a), CD4$^+$ (b), CD8$^+$ (c), and CD4$^-$CD8$^-$ (d) NKT cells (n = 3–6 female mice in each group). Representative data of three similar experiments are shown. The results are expressed as mean ± s.d. Statistical analysis was performed according to the Tukey-Kramer test. *$p<0.05$, **$p<0.01$.

doi:10.1371/journal.pone.0030568.g005

demonstrated the same tendency among the three mouse strains (data not shown). Of note, a higher MFI of CD1d expression was detected in the cells of the P1 population compared with the P2 population, both in WT and Jα18$^{-/-}$ mice (Figure 7C-a, b, c).

To examine functional differences in a specific Mϕ population, total cells from the SVF fraction were stimulated with LPS for 20 h and cytokines were measured (Figure 8). IL-10 levels were significantly higher in SVF cultures from CD1d$^{-/-}$ mice compared with WT mice (Figure 8A), and GM-CSF was significantly lower in Jα18$^{-/-}$ and CD1d$^{-/-}$ mice (Figure 8B). Notably, the production of TNF-α in the culture supernatant that could affect insulin resistance was not significantly different among the three strains (Figure 8C).

Glucose and insulin tolerance are ameliorated CD1d$^{-/-}$ mice

Since the pattern of adiposity should reflect levels of glucose intolerance, IPGTT was performed in the three mouse strains (Figure 9). No difference was observed in fasting blood sugar levels and in elevation after *i.p.* administration of glucose over time in the three strains fed an SFD (Figure 9A, left). On the other hand, CD1d$^{-/-}$ mice demonstrated the lowest fasting blood sugar level and a suppressed elevation profile after glucose administration among the three strains on an HFD (Figure 9A, right). Insulin levels were significantly higher in WT and Jα18$^{-/-}$ mice before and at 120 min after infusion than that obtained in the respective groups on an SFD (data not shown) and for CD1d$^{-/-}$ mice on an HFD, suggesting that insulin resistance was present in those strains (Figure 9B). To further examine insulin resistance, an ITT was performed in HFD-fed mice that had been fasted for 3.5 h [6] (Figure 9C). Following injection of insulin, blood glucose levels fell most prominently in CD1d$^{-/-}$ mice at 30 and 60 min after the injection (Figure 9C). The decrease in glucose level in WT mice injected with α-GalCer was less than that of mice injected with vehicle (Figure S1B), suggesting that insulin resistance was reproduced in mice when iNKT cells were activated [18], although there was no net increase in BW with the treatment. Thus, CD1d$^{-/-}$ mice developed the least resistance to insulin in the absence of both iNKT and type II NKT cells.

To examine whether type II NKT cells alone could reproduce the pathophysiological status observed in Jα18$^{-/-}$ mice, HMNC obtained from either Jα18$^{-/-}$ or CD1d$^{-/-}$ mice were intravenously transferred to CD1d$^{-/-}$ recipient mice and weight gain was examined on an HFD. CD1d$^{-/-}$ mice that received HMNC from Jα18$^{-/-}$ mice showed a slight increase in BW and exhibited a less profound decrease in blood glucose levels in the ITT (Figure S4A, C). Although no significant difference was detected with the IPGTT (Figure S4B), CD1d$^{-/-}$ mice that received HMNC from

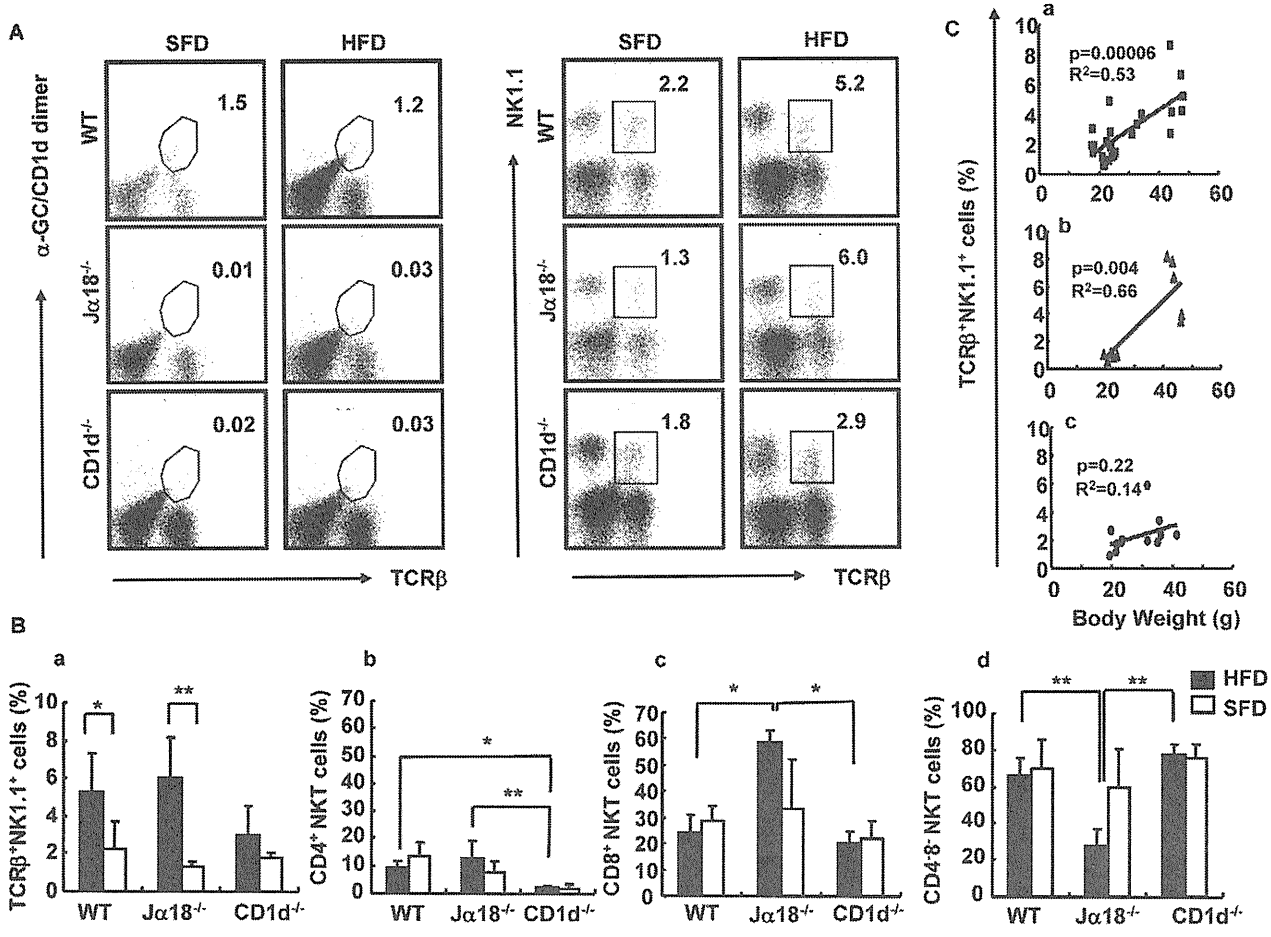

Figure 6. Flow cytometric analyses of NKT cells in adipose tissue in mice fed an SFD or an HFD. (A) A representative flow cytometric dot-plot defining the population of α-GalCer/CD1d dimer$^+$TCRβ$^+$ and NK1.1$^+$TCRβ$^+$ cells in adipose tissue of SFD-fed mice (a, c) and HFD-fed mice (b, d). (B) The proportion of each subset in SVF. NK1.1$^+$TCRβ$^+$ cells (a), CD4$^+$ (b), CD8$^+$ (c), and CD4$^-$CD8$^-$ (d) NKT cells (n = 3–6 female mice in each group). Representative data of three similar experiments are shown. The results are expressed as mean ± s.d. Statistical analysis was performed according to the Tukey-Kramer test. *$p<0.05$, **$p<0.01$. (C) The correlation between BW and the percentage of NKT cells in SVF by Pearson's correlation coefficient (R^2) test. WT (a), $P = 0.000006$; Jα18$^{-/-}$ (b), $P = 0.004$; and CD1d$^{-/-}$ (c), $P = 0.2$. Values with $P<0.05$ were considered statistically significant.
doi:10.1371/journal.pone.0030568.g006

Jα18$^{-/-}$ mice showed higher insulin resistance than CD1d$^{-/-}$ mice that received HMNC from CD1d$^{-/-}$ mice. The percentage of NKT cells (NK1.1$^+$ TCRβ$^+$) and CD4$^+$ NKT cells was similar in the liver and adipose tissue of CD1d$^{-/-}$ hosts (Figure S4D-a, b). However, CD8$^+$ NK1.1$^+$ T cells in adipose tissue were significantly increased in mice transferred with HMNC from Jα18$^{-/-}$-mice (Figure S4D-c), similarly to what we observed in Jα18$^{-/-}$ mice fed an HFD.

Discussion

Adipocytes, Mφ and T cells are now thought to constitute a functional triad to promote obesity and obesity-associated disorders [1–3,6–8]. Recently, the involvement of eosinophils and B cells has also been demonstrated [24,25], implying that many other immune cells participate in the physiologic and pathologic processes of adipocyte hypertrophy. This may be a natural process since adipose tissue is thought to be an ancestor of lymphoid organs [5,14].

In the present study, we demonstrated that an innate lymphocyte of the T cell lineage, the CD1d-restricted NKT cell, also has an active role in the development of obesity. When fed an HFD (CLEA Japan), CD1d$^{-/-}$ mice gained the least weight compared to Jα18$^{-/-}$ and WT mice. This difference was demonstrated when mainstream CD8$^+$ T cells were primarily unaffected. Furthermore, similar results were obtained with different types of HFD (Harlan Teklad [26] and our own original preparation [18]), suggesting that the suppression of weight gain was solely dependent on the deficiency of CD1d-restricted NKT cells but not on the specific source of fat, i.e. fatty acid composition.

Since Jα18$^{-/-}$ mice gained comparable BW as WT mice, the residual CD1d-restricted, type II NKT cells appeared to contribute to the accumulation of visceral fat in the body. In HFD-fed WT and Jα18$^{-/-}$ mice, the number of NK1.1$^+$TCRβ$^+$ cells increased along with the hypertrophic change of abdominal WAT (Figure 4, 6), whereas the α-GalCer-CD1d dimer$^+$ population did not change in adipose tissue of WT mice, suggesting that the type II NKT cells were the major population affecting adipose tissue metabolism. Accordingly, the transfer of NKT cells from Jα18$^{-/-}$ mice to CD1d$^{-/-}$ mice resulted in weight gain and significant increase in insulin resistance (Figure S4). Both the percentage and the cell number of NK1.1$^+$TCRβ$^+$ cells in adipose tissue correlated with the BW weights in Jα18$^{-/-}$

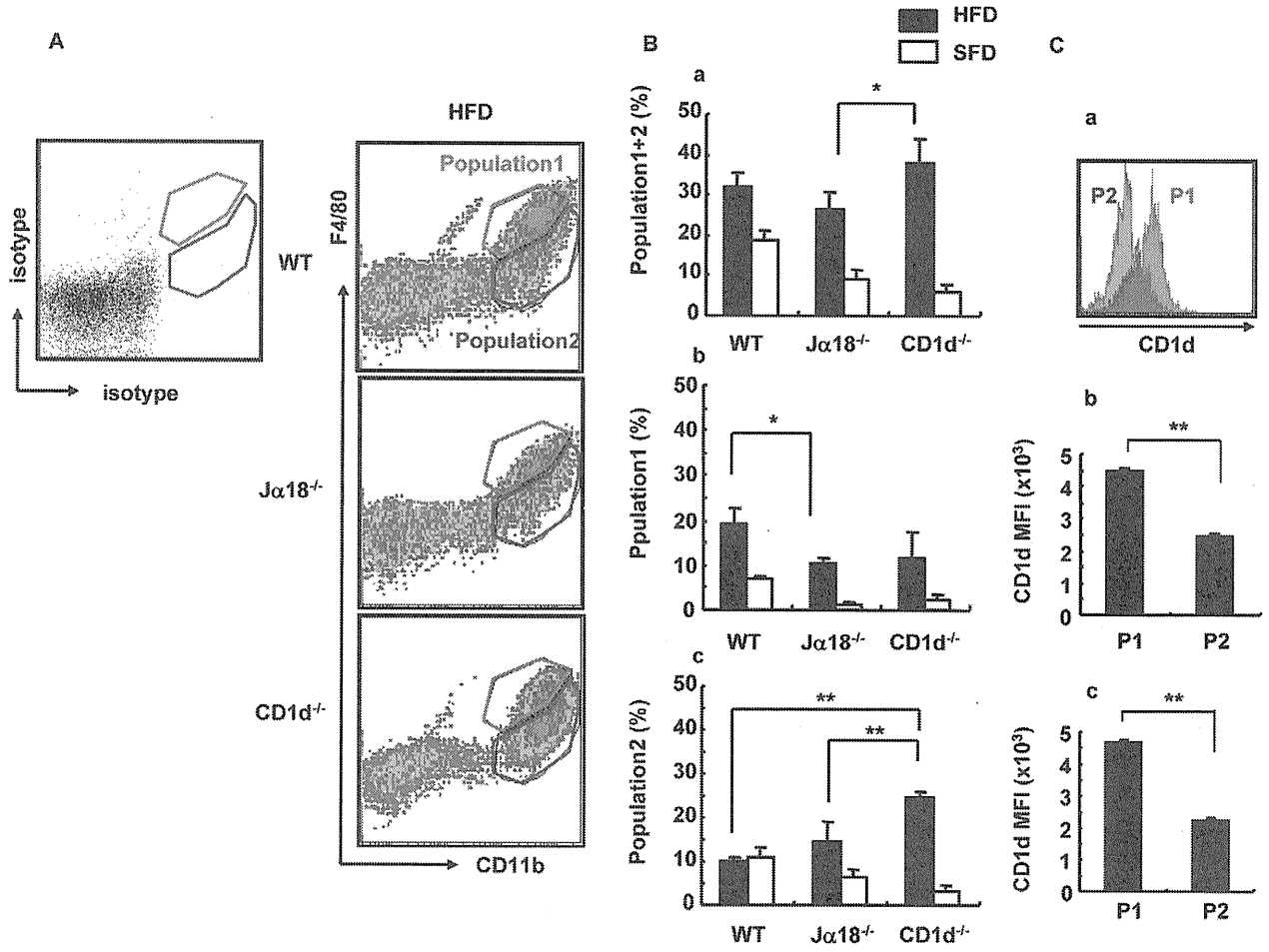

Figure 7. Flow cytometric analyses of infiltrated Mϕ in perigonadal adipose tissue. (A) A representative flow cytometric dot-plot defining the F4/80^{+}CD11b^{+} population in perigonadal adipose tissue in HFD-fed mice. F4/80^{hi} (Population 1; red gate) and F4/80$^{low~~}$ (Population 2; blue gate) are set to a staining with isotype control mAb. (B) The percentage of cells of CD11b^{+} (total) (a), Population 1 (b) and Population 2 (c). (C) CD1d expression by the Population 1 and Population 2 (a), MFI in WT (b) and Jα18$^{-/-}$ (c) mice fed an HFD (n = 3–4 male mice in each group). The results are expressed as mean ± s.d. Statistical analysis was performed according to the Tukey-Kramer test. *p<0.05, **p<0.01.
doi:10.1371/journal.pone.0030568.g007

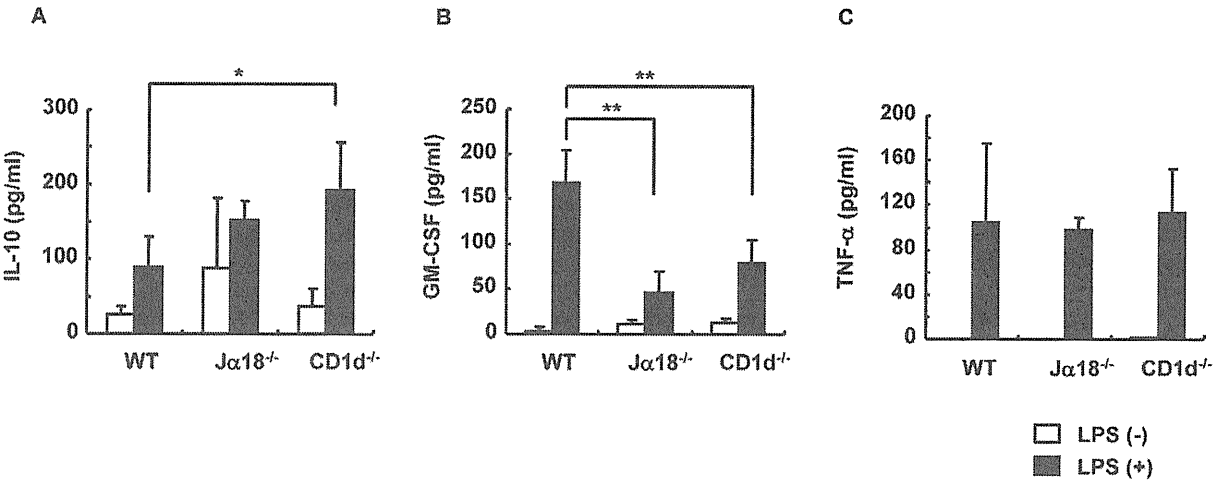

Figure 8. Cytokine production by Mϕ in perigonadal adipose tissue upon stimulation with LPS. (A–C) IL-10, GM-CSF and TNF-α concentrations after stimulation of Mφ in perigonadal adipose tissue with LPS (1 μg/ml) for 20 h (n = 3–4 male mice in each group). Representative data of three similar experiments are shown. The results are expressed as mean ± s.d. Statistical analysis was performed according to the Tukey-Kramer test. *p<0.05, **p<0.01.
doi:10.1371/journal.pone.0030568.g008

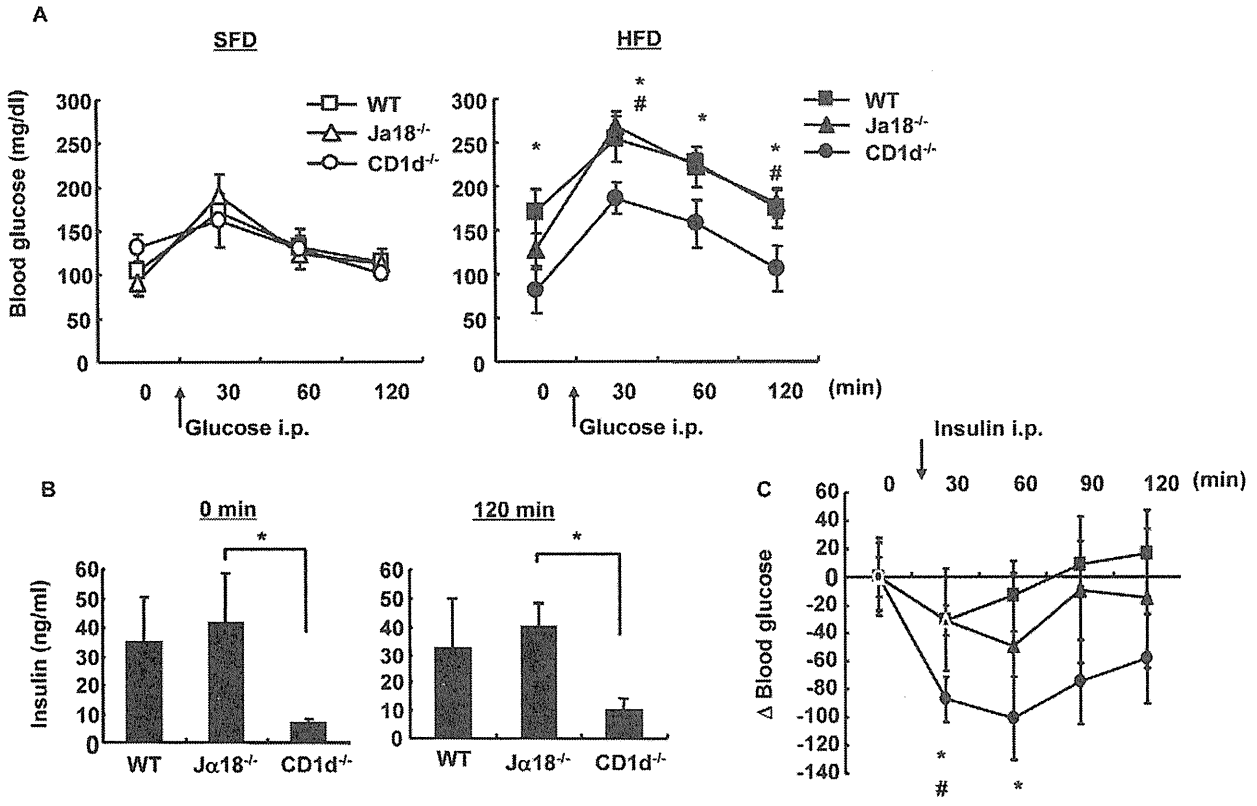

Figure 9. Glucose and insulin tolerance. (A) (IPGTT). Glucose (1 g/kg BW) was administered *i.p.* to female mice fed an SFD or an HFD. (B) The serum level of insulin 0 min and 120 min after glucose administration (*i.p.*) to HFD-fed mice was quantified by ELISA. (C) ITT. Insulin (0.75 U/kg BW) was administered *i.p.* to HFD-fed mice (n = 3–4 female mice in each group). Representative data of three similar experiments are shown. The results are expressed as mean ± s.d. Statistical analysis was performed according to the Tukey-Kramer test. *$p<0.05$ (WT versus CD1d$^{-/-}$); #$p<0.05$ (Jα18$^{-/-}$ versus CD1d$^{-/-}$).
doi:10.1371/journal.pone.0030568.g009

as well as in WT mice, whereas no correlation was found in CD1d$^{-/-}$ mice (Figure 6C). When the NK1.1^{+}TCRβ^{+} cells in adipose tissue were analyzed, we were unable to detect these cells with sulfatide-loaded CD1d-multimers that are specific for a subset of type II NKT cells [27] (data not shown). Of note, these cells exhibited a biased repertoire in specific Vβs in HFD-fed WT mice (data not shown), although the significance of this finding remains unclear. It should also be noted that α-GalCer administration did not boost weight gain in WT mice fed an HFD, although insulin action was blunted with α-GalCer administration. This result indicated that insulin resistance but not adiposity could be reproduced through the activation of type I NKT cells (Figure S1A).

Nishimura et al demonstrated that CD8^{+} T cells are important for recruitment of Mϕ and chronic inflammation in adipose tissue, which was proposed to propagate inflammation [6]. In our experiments, the CD8^{+} subset of NK1.1^{+} T cells, a rather rare subset [28], increased in adipose tissue in WT and Jα18$^{-/-}$ mice. Although we have not analyzed TCR Vβ chain usage, Nishimura described them as Vβ7 and Vβ10b [6]. Since Vβ7 is one of the preferred Vβ chains of NKT cells [29], it is possible that these cells or a portion of these cells include NKT cells. Very recently, Mantell et al. reported that no protection against metabolic abnormalities was noted in CD1d$^{-/-}$ mice fed an HFD [30]. They demonstrated no significant differences between WT and CD1d$^{-/-}$ mice in physiologic, metabolic, and inflammatory parameters. Nevertheless, since there was an early and reversible decrease in liver NKT cells, mice appeared to respond to an HFD. Specific reasons for these divergent findings will need to be explored in future studies. One possibility might be the colonization of mice from different animal facilities with different flora. An important role of intestinal flora in the process of obesity has emerged [31], and the differential dominance of certain species of microbes has been demonstrated in obese or anorexic human individuals [32]. Furthermore, in toll-like receptor 5 knockout (TLR5$^{-/-}$) mice, metabolic syndrome was induced by altered gut microbiota with hyperphagic traits [33]. Moreover, these metabolic changes could be conferred to WT, germ-free mice upon transfer of the gut microbiota derived from TLR5$^{-/-}$ mice. Although adaptive immunity is not directly related to the process of obesity in TLR5$^{-/-}$ mice, it should be noted that the development of adiposity could be controlled by balancing the complex microbiota. Since bacterial colonization in the intestine is regulated by a CD1d-dependent, NKT cell-mediated mechanism [34], it is possible that NKT cell deficiency may alter the intestinal flora, and thus influence either an adipogenic or anti-adipogenic host milieu.

The recruitment of Mϕ towards visceral fat, also known as adipose tissue Mϕ (ATMϕ; CD11b^{+}F4/80^{+}), has also been thought to be a hallmark of obesity [1,2]. The F4/80^{+} fraction can be subdivided into the F4/80^{high} and F4/80^{low} populations [35]. In the present study, ATMϕ of WT and Jα18$^{-/-}$ mice had an increased F4/80^{high} population, whereas CD1d$^{-/-}$ mice predominantly had an increased percentage and number of the

F4/80^{low} population. The F4/80^{high} population exhibits higher expression of TLR-4, TNF-α, and PPARγ than the F4/80^{low} population. Therefore, this subset represents pro-inflammatory Mϕ (M1) and accumulates in adipose tissue of obese mice [36]. On the other hand, the F4/80^{low} population exhibits higher IL-4 expression and represents anti-inflammatory Mϕ [36]. Furthermore, elimination of the F4/80^{high} population is associated with improved insulin sensitivity [37]. Our studies suggest that the predominance of F4/80^{high} ATMϕ is likely dependent on the presence of type II NKT cells, since it was observed in WT and Jα18$^{-/-}$ mice. Consistently, SVF that contained more F4/80^{low} Mϕ from CD1d$^{-/-}$ mice produced more IL-10 upon stimulation with LPS (Figure 8). The anti-inflammatory milieu induced by Mϕ polarization may ameliorate the development of obesity in CD1d$^{-/-}$ mice. It should also be noted that F4/80^{high} ATMϕ expressed higher levels of CD1d than F4/80^{low} Mϕ in WT and Jα18$^{-/-}$ mice, suggesting that NKT cells might better polarize these cells to cause adipose tissue inflammation. Alternatively, F4/80^{high} ATMϕ might express higher levels of CD1d as a result of the interaction with type II NKT cells.

The present study suggests that type II NKT cells may serve as a potential target for controlling the volume of visceral fat and insulin resistance. A possible approach may be the administration of a CD1d-binding ligand to modulate NKT cell function. Indeed, Ilan's group has demonstrated that the administration of glucocerebroside (β-glucosylceramide; β-GlcCer) or the direct transfer of NKT cells ameliorated metabolic aberration and steatohepatitis of leptin-deficient *ob/ob* mice [38,39]. They demonstrated that the therapeutic effects of β-GlcCer were associated with a Th2-shift (decreased IFN-γ and increased IL-10) and the redistribution of NKT cells in the liver to the periphery. Furthermore, β-GlcCer modulated the lipid rafts of NKT cells, thus altering the expression of molecules of cellular signaling, such as flotillin-2, Lck, and STAT1 [40]. Although the mode of action appears to be dependent on iNKT cells, it remains possible that these CD1d-binding non-stimulatory ligands may simply function as antagonists for all CD1d-restricted NKT cells.

Of special interest, Lynch et al. demonstrated that NKT cells and CD1d^{+} cells are abundantly detected in the omentum tissue in humans [41]. Half of the NKT (CD3^{+}CD56^{+}) cells stained with the 6B11 mAb [42], indicating that they were iNKT cells, but the remaining cells likely are type II NKT cells. They also reported a net decrease of iNKT cells in severely obese individuals with a relative increase of CD56^{+} T cells (healthy, 49.9%; obese, 61.9%) and discussed that the relative immunocompromised status in obesity due to the decreases in iNKT cells might be related to sensitivity to infections [40]. On the other hand, the omentum may be a source of not only iNKT cells but also type II NKT cells that are capable of inducing adiposity in the abdominal cavity.

In conclusion, we showed that deficiency of CD1d-resricted NKT cells suppressed the development of obesity, likely because inflammation of adipose tissue and liver were ameliorated and reduced levels of insulin resistance were induced. NKT cells, especially the type II subset, may be the initial subset of T cells that recognizes and responds to lipid excess. Thus, CD1d-restricted, type II NKT cells may be a novel target for therapeutic intervention in the metabolic syndrome. Searching for regulatory ligands and novel ways of regulation that include the selective elimination of pathogenic type II NKT cells might permit the control of not only metabolic syndrome but also various diseases related to lipid inflammation mediated by NKT cells [43].

Supporting Information

Figure S1 BW and insulin resistance of mice administered α-GalCer. (A) BW was determined weekly in WT mice given either vehicle or α-GalCer (0.1 μg/g BW). (B) ITT was performed for WT mice injected with vehicle or α-GalCer (n = 5 female mice in each group). Representative data of two similar experiments are shown. The results are expressed as mean ± s.d. Statistical analysis was performed according to the Student's *t*-test. *$p<0.05$.
(TIFF)

Figure S2 Serum T-chol-, HDL-chol, and TG levels. (A–C) Serum T-chol-, HDL-chol, and TG level after an 18 wk feeding and a 16 h fasting period (n = 6–8 female mice in each group). Representative data of three similar experiments are shown. The results are expressed as mean ± s.d. Statistical analysis was performed according to the Tukey-Kramer test. *$p<0.05$, **$p<0.01$.
(TIFF)

Figure S3 Dynamics of NKT cells in liver and adipose tissue during the early phase of feeding. The cell number of iNKT cells and NK1.1^{+}TCRβ^{+} cells in liver (A) and in adipose tissue (B) at 1, 2, 3, and 18 wk of HFD-feeding (n = 3–6 female mice in each group). Representative data of two similar experiments are shown. The results are expressed as mean ± s.d.
(TIFF)

Figure S4 Effects of adoptive transfer of Jα18$^{-/-}$ HMNC to CD1d$^{-/-}$ mice. (A) CD1d$^{-/-}$ mice received HMNC (1×10^{6}) from Jα18$^{-/-}$ mice since 8 wk of age on an HFD. BW was determined weekly. (B, C) IPGTT and ITT were performed at 14 wk of HFD feeding. (D) The number of NK1.1^{+}TCRβ^{+} cells (a) and the CD4/8 proportion in liver and adipose tissue (b, c) were analyzed by flow cytometry (n = 5 male mice in each group). Representative data of two similar experiments are shown. The results are expressed as mean ± s.d. Statistical analysis was performed according to Student's *t*-test. *$p<0.05$.
(TIFF)

Acknowledgments

We would like to thank Dr. Luc Van Kaer for sharing preliminary data and critically reading the manuscript. We are also grateful to Kirin Brewery Co., Ltd for kindly providing α-GalCer.

Author Contributions

Conceived and designed the experiments: YA MS NI HT KO KI. Performed the experiments: MS YA CSC HO NI KI KE. Analyzed the data: MS YA SF NH KE. Contributed reagents/materials/analysis tools: TN MT KE. Wrote the paper: MS KI.

References

1. Weisberg SP, McCann D, Desai M, Rosenbaum M, Leibel RL, et al. (2003) Obesity is associated with macrophage accumulation in adipose tissue. J Clin Invest 112: 1796–1808.
2. Xu H, Barnes GT, Yang Q, Tan G, Yang D, et al. (2003) Chronic inflammation in fat plays a crucial role in the development of obesity-related insulin resistance. J Clin Invest 112: 1821–30.
3. Kintscher U, Hartge M, Hess K, Foryst-Ludwig A, Clemenz M, et al. (2008) T-lymphocyte infiltration in visceral adipose tissue: a primary event in adipose tissue inflammation and the development of obesity-mediated insulin resistance. Arterioscler Thromb Vasc Biol 28: 1304–10.
4. Waki H, Tontonoz P (2007) Endocrine functions of adipose tissue. Annu Rev Pathol Mech Dis 2: 31–56.

5. Hotamisligil GS (2006) Inflammtion and metabolic disorders. Nature 444: 860–867.
6. Nishimura S, Manabe I, Nagasaki M, Eto K, Yamashita H, et al. (2009) $CD8^+$ T effector T cells contribute to macrophage recruitment and adipose tissue inflammation in obesity. Nat Med 15: 914–20.
7. Winer S, Chan Y, Palster G, Truong D, Tsui H, et al. (2009) Normalization of obesity-associated insulin resistance through immunotherapy. Nat Med 15: 921–9.
8. Feuerer M, Herrero L, Cipolletta D, Naaz A, Wong J, et al. (2009) Lean, but not obese, fat is enriched for a unique population of regulatory T cells that affect metabolic parameters. Nat Med 15: 930–9.
9. Van Kaer L (2007) NKT cells: T lymphocytes with innate effector functions. Curr Opin Immunol 19: 354–364.
10. Kawano T, Cui J, Koezuka Y, Toura I, Kaneko Y, et al. (1997) CD1d-restricted and TCR-mediated activation of Vα14 NKT cells by glycosylceramides. Science 278: 1626–9.
11. Matsuda JL, Mallevaey T, Scott-Browne J, Gapin L (2008) CD1d-restricted iNKT cells, the 'Swiss-Army knife' of the immune system. Curr Opin Immunol 20: 358–68.
12. Gumperz JE, Roy C, Makowska A, Lum D, Sugita M, et al. (2000) Murine CD1d-restricted T cell recognition of cellular lipids. Immunity 12: 211–21.
13. Exley MA, Koziel MJ (2004) To be or not to be NKT: Natural killer T cells in the liver. Hepatology 40: 1033–40.
14. Caspar-Bauguil S, Cousin B, Galinier A, Segafredo C, Nibbelink M, et al. (2005) Adipose tissues as an ancestral immune organ: Site-specific change in obesity. FEBS Lett 579: 3487–92.
15. Tupin E, Nicoletti A, Elhage R, Rudling M, Ljunggren HG, et al. (2004) CD1d-dependent activation of NKT cells aggravates atherosclerosis. J Exp Med 199: 417–422.
16. Nakai Y, Iwabuchi K, Fujii S, Ishimori N, Dashtsoodol N, et al. (2004) Natural killer T cells accelerate atherogenesis in mice. Blood 104: 2051–2059.
17. Major AS, Wilson MT, McCaleb JL, Ru Su Y, Stanic AK, et al. (2004) Quantitative and qualitative differences in proatherogenic NKT cells in apolipoprotein E-deficient mice. Arterioscler Thromb Vasc Biol 24: 2351–2357.
18. Ohmura K, Ishimori N, Ohmura Y, Tokuhara S, Nozawa A, et al. (2010) Natural killer T cells are involved in adipose tissues inflammation and glucose intolerance in diet-induced obese mice. Arterioscler Thromb Vasc Biol 30: 193–199.
19. Hansen TH, Huang S, Arnold PL, Fremont DH (2007) Patterns of nonclassical MHC antigen presentation. Nat Immunol 8: 563–568.
20. Mendiratta SK, Martin WD, Hong S, Boesteanu A, Joyce S, et al. (1997) CD1d1 mutant mice are deficient in natural T cells that promptly produce IL-4. Immunity 6: 469–477.
21. Cui J, Shin T, Kawano T, Sato H, Kondo E, et al. (1997) Requirement for Vα14 NKT cells in IL-12-mediated rejection of tumors. Science 278: 1623–1626.
22. Watanabe H, Ohtsuka K, Kimura M, Ikarashi Y, Ohmori K, et al. (1992) Details of an isolation method for hepatic mononuclear cells in mice. J Immunol Methods 146: 145–154.
23. Ogawa Y, Masuzaki H, Hosoda K, Aizawa-Abe M, Suga J, et al. (1999) Increased glucose metabolism and insulin sensitivity in transgenic skinny mice overexpressing leptin. Diabetes 48: 1822–9.
24. Wu D, Molofsky AB, Liang HE, Ricardo-Gonzalez RR, Jouihan HA, et al. (2011) Eosinophils sustain adipose alternatively activated macrophages associated with glucose homeostasis. Science 332: 243–7.
25. Winer DA, Winer S, Shen L, Wadia PP, Yantha J, et al. (2011) B cells promote insulin resistance through modulation of T cells and production of pathogenic IgG antibodies. Nat Med 17: 610–7.
26. Miyazaki Y, Iwabuchi K, Iwata D, Miyazaki A, Kon Y, et al. (2008) Effect of western diet on NKT cell function and NKT cell-mediated regulation of Th1 response. Scand J Immunol 67: 230–237.
27. Jahng A, Maricic I, Aguilera C, Cardell S, Halder RC, et al. (2004) Prevention of autoimmunity by targeting a distinct, noninvariant CD1d-reactive T cell population reactive to sulfatide. J Exp Med 199: 947–957.
28. Schümann J, Voyle RB, Wei BY, MacDonald HR (2003) Influence of the TCR Vβ domain on the avidity of CD1d: α-galactosylceramide binding by invariant Vα14 NKT cells. J Immunol 170: 5815–9.
29. Hammond KJ, Pelikan SB, Crowe NY, Randle-Barrett E, Nakayama T, et al. (1999) NKT cells are phenotypically and functionally diverse. Eur J Immunol 29: 3768–81.
30. Mantell BS, Stefanovic-Racic M, Yang X, Dedousis N, Sipula IJ, et al. (2011) Mice lacking NKT cells but with a complete complement of CD8 T-cells are not protected against the metabolic abnormalities of diet-induced obesity. PLoS One 6: e19831.
31. Bäckhed F, Ding H, Wang T, Hooper LV, Koh GY, et al. (2004) The gut microbiota as an environmental factor that regulates fat storage. Proc Natl Acad Sci U S A 101: 15718–23.
32. Armougom F, Henry M, Vialettes B, Raccah D, Raoult D (2009) Monitoring bacterial community of human gut microbiota reveals an increase in *Lactobacillus* in obese patients and *Methanogens* in anorexic patients. PLoS One 4: e7125.
33. Vijay-Kumar M, Aitken JD, Carvalho FA, Cullender TC, Mwangi S, et al. (2010) Metabolic syndrome and altered gut microbiota in mice lacking Toll-like receptor 5. Science 328: 228–231.
34. Nieuwenhuis EE, Matsumoto T, Lindenbergh D, Willemsen R, Kaser A, et al. (2009) Cd1d-dependent regulation of bacterial colonization in the intestine of mice. J Clin Invest 119: 1241–50.
35. Bassaganya-Riera J, Misyak S, Guri AJ, Hontecillas R (2009) PPARγ is highly expressed in $F4/80^{hi}$ adipose tissue macrophages and dampens adipose-tissue inflammation. Cell Immunol 258: 138–46.
36. Guri AJ, Hontecillas R, Ferrer G, Casagran O, Wankhade U, et al. (2008) Loss of PPARγ in immune cells impairs the ability of abscisic acid to improve insulin sensitivity by suppressing monocyte chemoattractant protein-1 expression and macrophage infiltration into white adipose tissue. J Nutr Biochem 19: 216–228.
37. Lumeng CN, Bodzin JL, Saltiel AR (2007) Obesity induces a phenotypic switch in adipose tissue macrophage polarization. J Clin Invest 117: 175–84.
38. Elinav E, Pappo O, Sklair-Levy M, Margalit M, Shibolet O, et al. (2006) Adoptive transfer of regulatory NKT lymphocytes ameliorates non-alcoholic steatohepatitis and glucose intolerance in ob/ob mice and is associated with intrahepatic CD8 trapping. J Pathol 209: 121–8.
39. Margalit M, Shalev Z, Pappo O, Sklair-Levy M, Alper R, et al. (2006) Glucocerebroside ameliorates the metabolic syndrome in OB/OB mice. J Pharmacol Exp Ther 319: 105–10.
40. Lalazar G, Ya'acov AB, Lador A, Livovsky DM, Pappo O, et al. (2008) Modulation of intracellular machinery by β-glycolipids is associated with alteration of NKT lipid rafts and amelioration of concanavalin-induced hepatitis. Mol Immunol 45: 3517–25.
41. Lynch L, O'Shea D, Winter DC, Geoghegan J, Doherty DG, et al. (2009) Invariant NKT cells and $CD1d^+$ cells amass in human omentum and are depleted in patients with cancer and obesity. Eur J Immunol 39: 1893–1901.
42. Exley MA, Hou R, Shaulov A, Tonti E, Dellabona P, et al. (2008) Selective activation, expansion, and monitoring of human iNKT cells with a monoclonal antibody specific for the TCR α-chain CDR3 loop. Eur J Immunol 38: 1756–66.
43. Roy KC, Maricic I, Khurana A, Smith TR, Halder RC, et al. (2008) Involvement of secretory and endosomal compartments in presentation of an exogenous self-glycol lipid to type II NKT cells. J Immunol 180: 2942–50.

Interleukin 6 signaling promotes anti-aquaporin 4 autoantibody production from plasmablasts in neuromyelitis optica

Norio Chihara[a,b], Toshimasa Aranami[a,c], Wakiro Sato[a], Yusei Miyazaki[a], Sachiko Miyake[a,c], Tomoko Okamoto[c,d], Masafumi Ogawa[c,d], Tatsushi Toda[b], and Takashi Yamamura[a,c,1]

[a]Department of Immunology, National Institute of Neuroscience, National Center of Neurology and Psychiatry (NCNP), Tokyo 187-8502, Japan; [b]Department of Neurology, Kobe University Graduate School of Medicine, Kobe 650-0017, Japan; and [c]Multiple Sclerosis Center and [d]Department of Neurology, National Center Hospital, NCNP, Tokyo 187-8551, Japan

Edited* by Tadamitsu Kishimoto, Graduate School of Frontier Biosciences, Osaka University, Suita, Japan, and approved January 26, 2011 (received for review November 21, 2010)

Neuromyelitis optica (NMO) is an inflammatory disease affecting the optic nerve and spinal cord, in which autoantibodies against aquaporin 4 (AQP4) water channel protein probably play a pathogenic role. Here we show that a B-cell subpopulation, exhibiting the $CD19^{int}CD27^{high}CD38^{high}CD180^{-}$ phenotype, is selectively increased in the peripheral blood of NMO patients and that anti-AQP4 antibodies (AQP4-Abs) are mainly produced by these cells in the blood of these patients. These B cells showed the morphological as well as the phenotypical characteristics of plasmablasts (PB) and were further expanded during NMO relapse. We also demonstrate that interleukin 6 (IL-6), shown to be increased in NMO, enhanced the survival of PB as well as their AQP4-Ab secretion, whereas the blockade of IL-6 receptor (IL-6R) signaling by anti–IL-6R antibody reduced the survival of PB in vitro. These results indicate that the IL-6–dependent B-cell subpopulation is involved in the pathogenesis of NMO, thereby providing a therapeutic strategy for targeting IL-6R signaling.

neuroinflamatory disease | autoimmunity | multiple sclerosis | central nervous system | IL-6 receptor blockade

Neuromyelitis optica (NMO) is an inflammatory demyelinating disorder characterized by recurrent attacks of severe optic neuritis and myelitis. Unlike the conventional form of multiple sclerosis (CMS), the lesions of NMO tend to spare the cerebral white matter, especially during the early stage (1), and even a single episode of attack can cause serious neurological deficits such as total blindness and paraplegia. Accordingly, accumulation of irreversible damage to the central nervous system (CNS) along with rapid progression of disability is more frequently found in NMO compared with CMS (2).

NMO can be distinguished from CMS by clinical, neuroimaging, and serological criteria (3). It is now known that serum anti-aquaporin 4 (AQP4) autoantibodies can be used as a disease marker of NMO (1, 2). AQP4 is the most abundantly expressed water channel protein in the CNS and is highly expressed in the perimicrovessel astrocyte foot processes, glia limitans, and ependyma (4). Emerging clinical and pathological observations suggest that anti-AQP4 antibodies (AQP4-Abs) play a key role in the pathogenesis of NMO. Prior studies have documented a significant correlation of serum AQP4-Ab levels with the therapeutic efficacy of plasma exchange during clinical exacerbations of NMO (2, 5). In the CNS lesions of NMO, reduced expression of AQP4 on astrocytes is evident even during the early stage (6), which is followed by the occurrence of vasculocentric destruction of astrocytes associated with perivascular deposition of complement and IgG (7).

On the other hand, recent studies have suggested that AQP4-Abs alone are incapable of causing the clinical and pathological features of NMO. In fact, Hinson et al. emphasized the role of cellular immunity in combination with AQP4-Abs by showing that the attack severity of NMO was not correlated with serum AQP4-Ab levels (8). It was also demonstrated that direct injection of IgGs derived from NMO patients into the brains of naïve mice did not cause NMO-like lesions, although brain tissue destruction associated with leukocyte infiltration was elicited by coinjecting human complement (9). Other groups have shown that the passive transfer of IgGs from NMO patients to rats challenged with induction of experimental autoimmune encephalomyelitis (EAE) may cause a decrease in the expression of AQP4 in astrocytes along with worsening of clinical EAE (10–12). In contrast, the transfer of IgGs to unimmunized rats did not cause any pathology. These results suggest that induction of AQP4-Ab–mediated pathology in NMO depends on the presence of complement, leukocytes, and T cells.

Although AQP4-Ab–secreting cells are a potential target for therapy, detailed characteristics of AQP4-Ab–producing cells have not been clarified yet. Because some NMO patients have elevated serum anti-nuclear and anti–SS-A/SS-B Abs (1), as found in patients with systemic lupus erythematosus (SLE) or Sjögren syndrome, NMO might share common pathological mechanisms with these autoimmune diseases. Kikuchi et al. previously reported that $CD180^{-}$ B cells are activated B cells capable of producing autoantibodies in SLE (13). CD180 is a member of the leucine-rich repeat family of molecules with homology to Toll-like receptor 4 (14), which is highly expressed by naïve and memory B cells but not by plasma cells (15). Odendahl et al. demonstrated that $CD27^{high}CD38^{+}$ B cells, capable of producing high-affinity IgG (16), are increased in the peripheral blood of SLE patients with some correlation to disease activity (17). Considering the phenotypes of autoantibody-producing cells reported in SLE, we analyzed the expression of CD27, CD38, and CD180 on $CD19^{+}$ B cells in the peripheral blood of NMO patients. We found that $CD27^{high}CD38^{high}CD180^{-}$ B cells were significantly increased in AQP4-Ab seropositive patients diagnosed with NMO or NMO spectrum disorder (1) compared with healthy subjects (HS) or CMS patients. Notably, this B-cell subpopulation was found to be a major source of AQP4-Abs in the peripheral blood of AQP4-Ab seropositive patients and depended on interleukin-6 receptor (IL-6R) signaling for survival.

IMMUNOLOGY

Author contributions: N.C., T.A., S.M., and T.Y. designed research; N.C. and W.S. performed research; Y.M. and S.M. contributed new reagents/analytic tools; N.C., T.A., T.O., M.O., T.T., and T.Y. analyzed data; T.Y. supervised the work; and N.C., T.A., and T.Y. wrote the paper.

The authors declare no conflict of interest.

*This Direct Submission article had a prearranged editor.

Freely available online through the PNAS open access option.

[1]To whom correspondence should be addressed. E-mail: yamamura@ncnp.go.jp.

This article contains supporting information online at www.pnas.org/lookup/suppl/doi:10.1073/pnas.1017385108/-/DCSupplemental.

Results

$CD27^{high}CD38^{high}CD180^{-}$ B Cells Were Increased in the Peripheral Blood of NMO Patients. Although AQP4-Abs are identified as IgGs (18), no prior study has focused on proportional changes of B-cell subsets in NMO. We therefore performed multicolor flow cytometric analysis of peripheral blood mononuclear cells (PBMC) derived from patients and controls. After starting the study, we soon noticed a remarkable expansion of a distinct B-cell subset in some patients with NMO. The expanded B cells were identified as a population of $CD27^{high}$, $CD38^{high}$, and $CD180^{-}$, and showed lower expression of CD19 than other B cells (Fig. 1*A*). Notably, this population did not express the B-cell marker CD20 (Fig. S1). First, we collected samples from patients in remission and analyzed the pooled data. We found that the proportion of this subpopulation among $CD19^{+}$ B cells was significantly increased in AQP4-Ab seropositive patients with NMO or NMO spectrum disorder (Fig. 1*B*) compared with HS or CMS patients. There was no significant difference in the proportion of this B-cell subpopulation between those with typical NMO and those with NMO spectrum disorder. Furthermore, the frequency of this B-cell subpopulation was correlated with the serum AQP4-Ab titer (Fig. S2). Comparison of paired samples obtained from the same patients during relapse and in remission showed that the $CD27^{high}CD38^{high}CD180^{-}$ B cells further increased during relapse (Fig. 1*C*). In contrast, the frequencies of $CD27^{-}$ naïve B cells (nB) and $CD27^{+}CD38^{-low}$ memory B cells (mB) were not altered in AQP4-Ab seropositive patients compared with controls (Fig. S3). The large majority of seropositive patients were treated with corticosteroids. However, the frequency of $CD27^{high}CD38^{high}CD180^{-}$ cells among $CD19^{+}$ B cells was not correlated with the daily corticosteroid dose given to patients (Fig. S4). Moreover, the increase in cells in NMO patients was still evident compared with that in CMS patients similarly treated with corticosteroids (Fig. S5). Taken together, the selective increase in $CD27^{high}CD38^{high}CD180^{-}$ B cells in seropositive patients was thought to reflect their role in the pathogenesis of NMO but not to be an effect of the corticosteroid treatment.

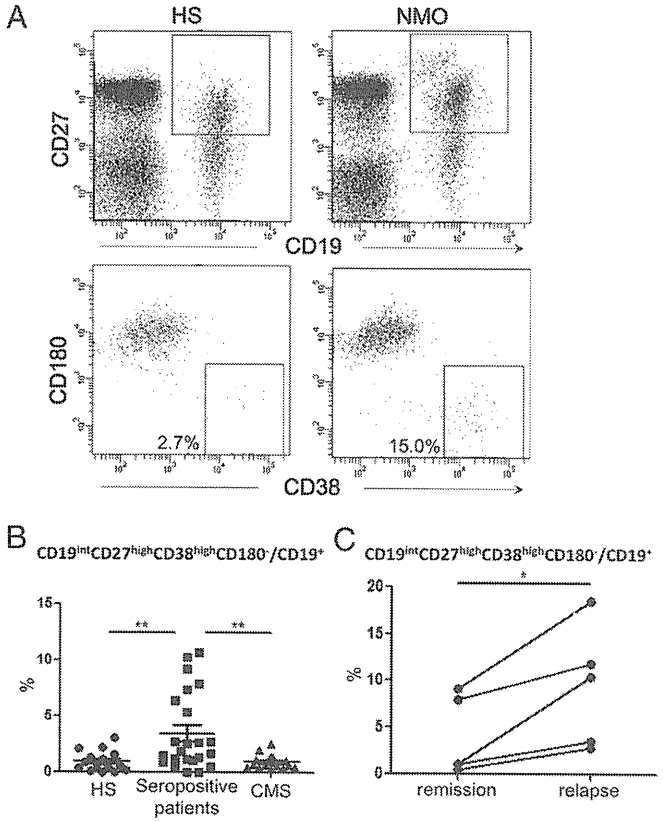

Fig. 1. $CD27^{high}CD38^{high}CD180^{-}$ B cells increased in NMO patients. (*A*) A flow cytometric scheme for the analysis of B-cell subpopulations. PBMC from HS and NMO in remission were stained with fluorescence-conjugated anti-CD19, -CD27, -CD38, and -CD180 mAbs. $CD19^{+}CD27^{+}$ cells were partitioned (*Upper*) and analyzed for expression of CD38 and CD180 (*Lower*). Values represent the percentage of $CD38^{high}CD180^{-}$ cells within $CD19^{+}CD27^{+}$ cells. (*B*) Analysis of the pooled data derived from patients in clinical remission. This shows the percentages of $CD27^{high}CD38^{high}CD180^{-}$ cells within $CD19^{+}$ cells from HS, seropositive patients, and CMS patients (**$P < 0.01$; Tukey's post hoc test). (*C*) Comparison of remission and relapse of NMO. Data obtained from the same patients are connected with lines (*$P < 0.05$; Wilcoxon signed rank test).

Expanded Cells Resemble Early Plasma Cells in Gene Expression and Morphology. To gain insights into the developmental stage of the $CD27^{high}CD38^{high}CD180^{-}$ B cells, we quantified the mRNA expression of B-cell–associated transcription factors in sorted cell populations. Compared with nB and mB, this population showed much higher expression of B-lymphocyte-induced maturation protein 1 (Blimp-1) and IFN regulatory factor 4 (IRF4), which are essential for the regulation of plasma cell differentiation (19, 20) (Fig. 2*A*). In contrast, the expression of paired box gene 5 (PAX5), known to be down-regulated in early plasma cell differentiation (21), was reciprocally reduced in the B-cell subset. This gene expression pattern is very similar to that of plasma cells. However, it was notable that the cells of interest expressed CD19, which is not detected in mature plasma cells. Moreover, only 40% of this population expressed the most reliable plasma cell marker CD138 (22). Morphological analysis also confirmed the similarity of this population to plasma cells: they exhibit eccentric nucleus, perinuclear hof region, and abundant cytoplasm. However, they possess a larger nucleus with a lower extent of chromatin clumping compared with $CD138^{+}$ plasma cells derived from HS (Fig. 2*B*). Notably, the $CD138^{+}$ population among $CD27^{high}CD38^{high}CD180^{-}$ cells in NMO patients was

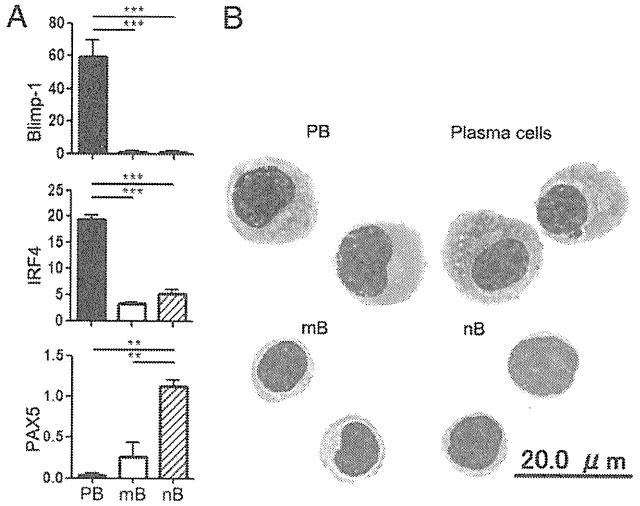

Fig. 2. Resemblance of $CD19^{int}CD27^{high}CD38^{high}CD180^{-}$ cells to plasma cells. (*A*) mRNA expression of Blimp-1, IRF4, and PAX5. B-cell subpopulations [$CD27^{high}CD38^{high}CD180^{-}$ (PB), $CD27^{-}$ naïve (nB), $CD27^{+}CD38^{-low}$ memory (mB)] were sorted by FACS and total RNA was extracted for qRT-PCR analysis. RNA levels were normalized to ACTB for each sample (**$P < 0.01$; ***$P < 0.001$; Tukey's post hoc test). (*B*) May–Grünwald–Giemsa staining of B-cell subpopulations. PB (*Upper Left*), mB (*Lower Left*), and nB (*Lower Right*) from NMO are presented along with morphologically identified plasma cells ($CD19^{int}CD27^{high}CD38^{high}CD138^{+}$) from HS (*Upper Right*).

morphologically indistinguishable from the $CD138^-$ population in NMO patients or HS, indicating the immature characteristic of $CD27^{high}CD38^{high}CD180^-$ cells (Fig. S6). These phenotypical and morphological characteristics as well as the results of the quantitative real-time PCR (qRT-PCR) analysis indicate that this B-cell population is equivalent to plasmablasts (PB) (22–26). Hereafter, we use the term "PB" to distinguish this population from other B cells.

Expression of B-Cell Cytokine Receptors on PB. Prior studies have identified cytokines that are critically involved in the differentiation and/or survival of plasma cells, including IL-6 and B-cell–activating factor (BAFF). IL-6 induces B-cell differentiation into plasma cells, maintains early plasma cell survival, and enhances plasma cell IgG secretion (24). Besides, IL-6 is elevated in the cerebrospinal fluid (CSF) or peripheral blood of NMO patients compared with that of CMS patients and HS (27, 28). In a rodent autoimmunity model, IL-6 deficiency caused impaired autoantibody secretion by B cells (29). Given the potential role of IL-6 in NMO, we performed flow cytometry analysis for the expression of IL-6R. Results showed remarkable expression of IL-6R on PB, although it was only marginal or absent on mB and nB (Fig. S7). Because BAFF and A proliferation-inducing ligand (APRIL) can also promote the survival of PB (25, 26), we next evaluated the expression of the receptors for BAFF and APRIL, BAFF receptor (BAFF-R), B-cell maturation antigen (BCMA), and transmembrane activator and calcium modulator and cyclophilin ligand interactor (TACI). Expression of BCMA and TACI was selectively up-regulated in PB in parallel with IL-6R. In contrast, BAFF-R was up-regulated in mB and nB, but not in PB (Fig. S7).

PB Is a Selective Source of AQP4-Abs in Peripheral Blood. We were interested to know whether PB were capable of producing AQP4-Abs upon stimulation with cytokines and, therefore, examined the ability of IL-6, BAFF, and APRIL to enhance AQP4-Ab secretion by PB. We cultured the isolated PB for 6 d in the presence or absence of each cytokine, and evaluated the presence of AQP4-Abs in the supernatants by measuring IgG binding to Chinese hamster ovary (CHO) cells transfected with the human AQP4 vector (CHO^{AQP4}) or the vector control (CHO^{VC}). We found that IL-6, but not BAFF or APRIL, could significantly enhance AQP4-Ab secretion from PB (Fig. S8), as assessed by specific IgG binding to CHO^{AQP4}. Further study focusing on IL-6 showed that exogenous IL-6 promoted the production of AQP4-specific IgGs from PB (Fig. 3*A*), but not from the other B-cell subpopulations. Similar results were obtained from six independent experiments (Fig. S9), indicating that PB could be major AQP4-Ab producers in PBMC. In the absence of addition of IL-6, supernatants from PB did not show any significant reactivity to CHO^{AQP4}. To further analyze the AQP4-Ab–secreting potential of each B-cell subpopulation, we next stimulated the cells with a combination of IL-6, IL-21, and anti-CD40 that efficiently induces B-cell differentiation and IgG production (30). This polyclonal stimulation induced the secretion of similar amounts of IgGs from mB and PB. However, only the supernatant of PB specifically reacted to CHO^{AQP4} cell transfectants, indicating that AQP4-Ab–producing B cells were highly enriched in PB (Fig. 3*B*).

Survival and Functions of PB Depend on IL-6 Signaling. We evaluated the influence of IL-6, BAFF, and APRIL on the survival of PB after 2 d of in vitro culture (Fig. 4*A*). Among the added cytokines, only IL-6 was found to significantly promote the survival of PB (Fig. 4*B*). We also assessed the expression levels of X-box-binding protein 1 (XBP-1) in PB by qRT-PCR after 24 h of culture with or without IL-6. XBP-1 is a transcription factor critical for IgG secretion (31), and the splicing process of XBP-1 mRNA yields a more active and stable protein. We found that the expression of both unspliced [XBP-1(u)] and spliced [XBP-1(s)] forms of XBP-1 mRNA was augmented in PB by the ad-

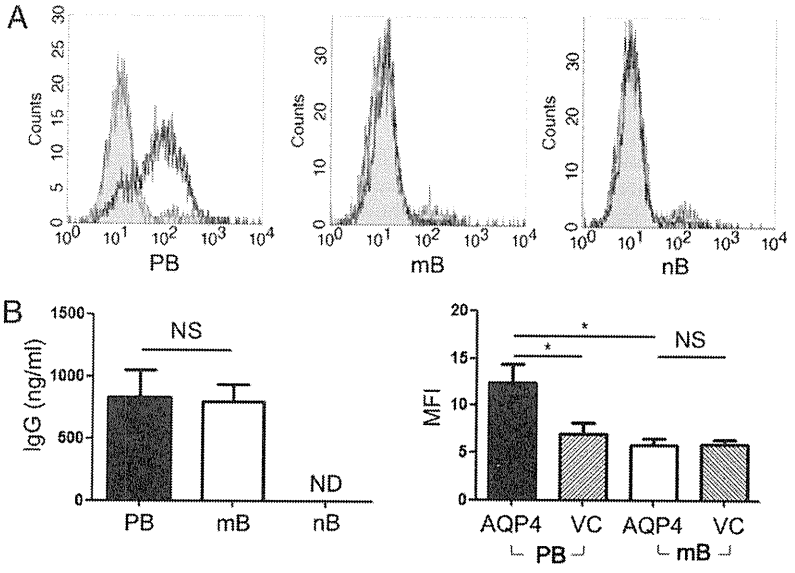

Fig. 3. Production of AQP4-Abs by PB. (*A*) Using flow cytometry, we examined whether AQP4-Abs could be produced by PB, mB, or nB cells. FACS-sorted cells were cultured with IL-6 (1 ng/mL) for 6 d and supernatants were collected. Supernatant IgGs reactive to CHO^{AQP4} (open histogram) and CHO^{VC} cells (closed histogram) were detected by anti-human IgG secondary antibody. The supernatant from PB (*Left*), but not from mB or nB, contains IgGs reactive to CHO^{AQP4}, indicating that only PB secrete AQP4-Abs after stimulation with IL-6. (*B*) Memory B cells (mB) produce IgGs but not AQP4-Abs. B-cell subpopulations were cultured in the presence of IL-6 (1 ng/mL), IL-21 (50 ng/mL), and anti-CD40 mAb (1 μg/mL) for 6 d. IgGs in the culture supernatants were measured by sandwich ELISA (*Left*) (each assay was performed in quadruplicate). Data from three patients are expressed as mean ± SD. The activity of AQP4-Abs in the culture supernatants from PB and mB was also measured by flow cytometry (*Right*). Aliquots of CHO^{AQP4} cells (AQP4) and CHO^{VC} cells (VC) ($n = 4$ for each) were stained with the supernatant of PB or mB from every patient. Data are expressed as median fluorescence intensity values from the results of three patients (*$P < 0.05$; Tukey's post hoc test). ND, not detected; NS, not significant.

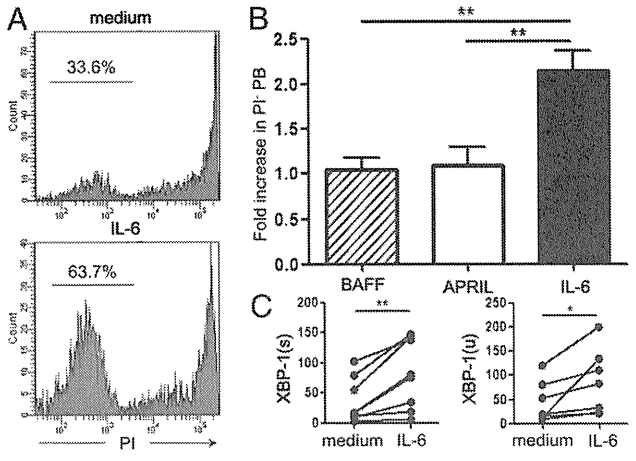

Fig. 4. Effect of exogenous IL-6 on PB. (*A*) IL-6 promotes the survival of PB. FACS-sorted PB were cultured in the presence or absence of recombinant IL-6 (1 ng/mL) for 2 d. PI staining of cultured PB showed that exogenous IL-6 increased the percentage of surviving cells (*Lower*) compared with cells cultured in the medium alone (*Upper*). Values shown are percentages of unstained cells. (*B*) Comparison of IL-6 with BAFF and APRIL. Here we show that only IL-6 could promote cell survival. Data are expressed as fold increase of % PI^- cells following the addition of each cytokine. At least four independent experiments were performed to obtain the results (**$P < 0.01$; Tukey's post hoc test). (C) Effect of IL-6 on XBP-1 expression. FACS-sorted PB were cultured with or without IL-6 for 24 h, and total RNA was extracted from the cells to quantify expression levels of XBP-1(u) and XBP-1(s) by qRT-PCR. Each line connects values obtained from seven independent experiments (*$P < 0.05$; **$P < 0.01$; Wilcoxon signed-rank test).

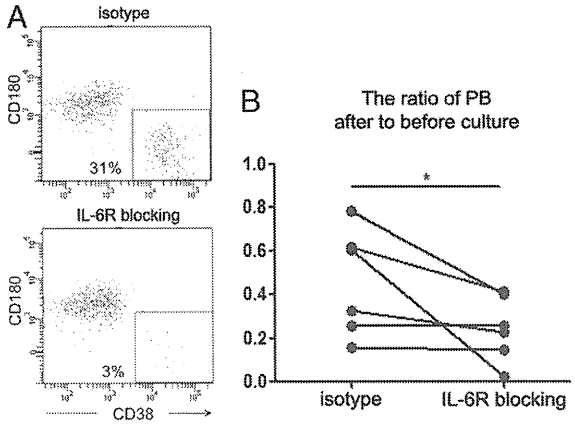

Fig. 5. IL-6R blockade selectively inhibits the survival of PB. (*A*) PBMC were cultured in a medium containing 20% autologous serum in the presence of IL-6R–blocking antibody or its isotype control mAb for 2 d. The cells were stained and analyzed as described in the experiment in Fig. 1*A*. Data represent the percentages of PB within $CD19^+CD27^+$ cells. A representative pair of six independent experiments is shown. (*B*) The percentage of PB within $CD19^+$ B cells (PB%) was determined for each pair of cultures either with anti–IL-6R mAb (IL-6R–blocking) or isotype control mAb (isotype) before and after starting the culture. Then, the PB survival ratio was calculated for each culture by dividing the PB% at the end of the culture by the PB% obtained before starting the culture. Lines connect the PB survival ratios of six independent experimental pairs to clarify that IL-6R blockade reduces PB survival (*$P < 0.05$; Wilcoxon signed-rank test).

dition of IL-6. These results suggest that IL-6 promoted the survival of PB and enhanced IgG secretion from PB, leading to an increased production of AQP4-Abs in NMO patients (Fig. 4*C*). In addition, we found that the frequency of PB tended to be increased when serum IL-6 levels were higher than the mean ± 2× SEM of those in HS [PB/PBMC (%) for IL-6 high group 0.62 ± 0.47 (%); PB/PBMC (%) for IL-6 low group 0.15 ± 0.05 (mean ± SD)]. These observations prompted us to address whether the blockade of IL-6R signaling could exhibit any influence on PB. We cultured PBMC derived from AQP4-Ab seropositive patients in the presence of 20% autologous serum and examined the effect of adding anti–IL-6R antibody by counting the number of surviving PB. We found that the frequency of PB among total B cells decreased significantly in the presence of anti–IL-6R mAb (Fig. 5 *A* and *B*). Among six patients examined, the PB reduction was remarkable in three patients, but was only marginal in the other patients. Notably, the former group of patients showed higher IL-6 levels in the serum (4.69, 6.47, and 25.5 pg/mL for each patient), compared with the latter (1.42, 1.43, and 2.91 pg/mL). The frequency of other B-cell subpopulations did not change with the addition of anti–IL-6R mAb. These results led us to postulate that in vivo administration of anti–IL-6R mAb may ameliorate NMO.

Discussion

A growing body of evidence suggests that AQP4-Abs play a pathogenic role in NMO (6, 7, 10–12). Here we report that a B-cell subpopulation bearing the $CD19^{int}CD27^{high}CD38^{high}CD180^-$ phenotype is responsible for the selective production of AQP4-Abs. The cells that we call PB are vulnerable to IL-6R blockade by anti–IL-6R mAb, leading us to propose anti–IL-6R mAb as a therapeutic option for NMO. Bennett et al. recently reported that plasma cells in CSF are a potential source of pathogenic AQP4-Abs (10). However, this study has not excluded a possible role of AQP4-Abs produced in the peripheral blood. It has been repeatedly shown that the passive transfer of pathogenic autoantibodies, including AQP4-Abs (10–12, 32), augments the formation of inflammatory lesions in EAE. Therefore, once T-cell–mediated inflammation takes place in the CNS, pathogenic autoantibodies produced outside the CNS are able to enter the CNS compartment. It is also notable that AQP4-Abs are more abundant in the peripheral blood of NMO patients than in their CSF (33). Taken together, we speculate that PB that are expanded in the peripheral blood during relapse may play a critical role in the pathogenesis of NMO by producing AQP4-Abs, although more work is necessary to explore whether PB can enter the CNS.

It is generally thought that circulating IgGs are mainly secreted by long-lived plasma cells residing in healthy bone marrow. It remains unclear how PB secreting AQP4-Abs can differentiate and survive in the peripheral circulation. It has been previously shown that autoantibodies producing plasma cells accumulate in peripheral lymphoid organs (34). It would be interesting to investigate which organs blood PB move to during the course of NMO. The levels of IL-6 in the serum and CSF are elevated in NMO compared with HS or CMS patients (27, 28). In this regard, it is of note that blocking IL-6R signaling was found to dramatically reduce the survival of PB ex vivo, which was dependent on the presence of autologous serum containing IL-6. These results suggest that the increase of PB in AQP4-Ab seropositive patients could be attributed to the increased IL-6 in the serum. We also demonstrated that improved PB survival in the presence of exogenous IL-6 was accompanied by up-regulated expression of XBP-1. It is noteworthy that wild-type and $XBP\text{-}1^{-/-}$ B cells start to produce more IL-6 after forced overexpression of XBP-1(s), which results in the operation of a positive feedback loop controlling IgG secretion (31). Treatment with anti–IL-6R is promising because IL-6R blockade could terminate this vicious loop that controls the production of autoantibodies.

It has been reported that NMO patients have higher levels of BAFF in the serum or CSF compared with CMS patients (35). BAFF is also known to support plasma cell differentiation and survival of PB induced in vitro (25). However, in our ex vivo

study, BAFF did not promote the survival of PB, indicating that PB were not a target for BAFF. We speculate that BAFF might specifically act on an early process of plasma cell differentiation and does not have an influence on cells like PB that have entered a later stage.

IL-6R blockade by humanized mAb against IL-6R (tocilizumab) has proven to be useful for treating immune-mediated diseases, including rheumatoid arthritis (36) and Castleman's disease (37). Here we propose that IL-6R–blocking antibody treatment should be considered as a therapeutic option for NMO. Currently, most NMO patients are being treated with corticosteroids in combination with immunosuppressive drugs and plasma exchange (38). Anti-CD20 mAb, which causes B-cell depletion, has also been used for serious cases of NMO. Because the level of B-cell depletion appears to correlate with the suppressive effects of anti-CD20 in NMO (39), it has been argued that B cells are essential for the pathogenesis of NMO, either via acting as antigen-presenting cells or as autoantibody producers. Weber et al. recently reported that activated antigen-specific B cells serve as antigen-presenting cells and polarize proinflammatory T cells in EAE (40), supporting the view that the therapeutic effects of anti-CD20 might be attributable to the depletion of antigen-presenting B cells. Notably, they also cautioned that elimination of $CD20^+$ cells might deplete nonactivated cells as well as regulatory B cells possessing anti-inflammatory potentials. Although the effect of anti-CD20 on AQP4-Ab–secreting cells has not been reported, it is likely that the majority of PB are not affected because they do not express CD20. Consistent with our prediction, anti-CD20 treatment was not effective in aggressive cases of NMO (41, 42). It appears that selective depletion of activated antigen-specific B cells could be a more promising strategy to improve the efficacy of B-cell–targeted therapies for NMO. In this regard, PB-targeting therapy is a promising approach. Given the efficacy of IL-6R blockade in reducing the number of PB ex vivo, we find it very interesting to explore the effect of anti–IL-6R mAb on NMO.

Materials and Methods

Patients and Controls. A cohort of 24 AQP4-Ab seropositive patients was recruited at the Multiple Sclerosis Clinic of the National Center of Neurology and Psychiatry (NCNP). Among these, 16 met the revised NMO diagnostic criteria (3). The other 8 were diagnosed with NMO spectrum disorder (1) because they did not develop both myelitis and optic neuritis (optic neuritis alone in 6 cases; myelitis alone in 2 cases). Seventeen age- and sex-matched CMS patients and 20 HS were enrolled as controls. Serum AQP4-Ab levels were measured by a previously reported protocol by courtesy of Kazuo Fujihara at Tohoku University (Sendai, Japan) (33). All CMS patients had relapsing-remitting MS and fulfilled McDonald diagnostic criteria (43).

At the time of blood sampling, 21 seropositive patients were receiving corticosteroids (prednisolone 5–25 mg/d). Seven of these patients were also being treated with azathioprine (12.5–100 mg/d) or tacrolimus (3 mg/d). Six CMS patients were receiving low-dose corticosteroids without immunosuppressants. None of the seropositive or CMS patients had received IFN-β, i.v. corticosteroids, plasma exchange, or i.v. immunoglobulins for at least 1 mo before blood sampling. Blood sampling during relapse was performed in six seropositive NMO patients before they received intensive therapy starting with i.v. corticosteroids. Five of these patients were followed up further and blood was collected again after they entered remission. Anti-nuclear and/or anti–SS-A Abs were detected in some of the seropositive patients, but none met the diagnostic criteria for SLE or Sjögren syndrome. Demographic features of the patients are presented in Table 1. The study was approved by the Ethics Committee of the NCNP.

Reagents. The following Abs were used in this study: mAbs against CD38, CD19, CD27, CD20, and PE-streptavidin (Beckman Coulter); mAbs against CD180 and BAFF-R (BD Biosciences); mAbs against IL-6R and TACI as well as Abs against BCMA and CD40 (R&D Systems); rabbit anti-human AQP4 antibody (Santa Cruz Biotechnology); FITC-anti-rabbit IgG (Jackson ImmunoResearch Laboratories); and FITC-anti-human IgG antibody (MP Biomedicals). Recombinant proteins of BAFF (ProSpec), APRIL (Abnova), IL-6 (PeproTech), and IL-21 (Invitrogen) were purchased. Propidium iodide (PI) was obtained from Sigma-Aldrich. RPMI 1640 supplemented with 10% FBS, 2 mM L-glutamine, 100 U/mL penicillin, and 100 mg/mL streptomycin (Life Technologies) was used for cell culture.

Flow Cytometry, Cytology, and Cell Culture. PBMC were separated using density centrifugation on Ficoll-Paque PLUS (GE Healthcare Biosciences). B cells were analyzed and sorted by FACSAria (BD Biosciences). Each B-cell subset was stained with May–Grünwald–Giemsa. To evaluate AQP4-Ab production in vitro, each B-cell subset (1 or 2×10^4) was cultured for 6 d in the medium alone, in the presence of IL-6 (1 ng/mL) or in the presence of IL-6 (1 ng/mL), IL-21 (50 ng/mL), and anti-CD40 (1 μg/mL). Culture supernatants were harvested and analyzed for AQP4-Ab production as described below. To examine the effect of cytokines on the survival of PB, the cells (4×10^3) were cultured in the medium alone or in the presence of BAFF (100 ng/mL), APRIL (300 ng/mL), or IL-6 (1 ng/mL) in 96-well U-bottom plates for 2 d and stained with PI to assess cell survival. In parallel, the cells were cultured for 1 d and harvested to evaluate mRNA expression by qRT-PCR. To assess the effect of IL-6 signaling blockade, PBMC (5×10^5) were preincubated with anti–IL-6R Abs (1 μg/mL) at 4 °C for 20 min, cultured in AIM-V medium (Invitrogen) containing 20% of heat-inactivated serum obtained from each patient in 96-well flat-bottom plates for 2 d, and analyzed by flow cytometry.

Quantitative RT-PCR Analysis. mRNA from each cell subset was isolated according to the manufacturer's instructions using an RNAeasy Kit (Qiagen). RNA was further treated with DNase using the RNase-Free DNase Set (Qiagen) and reverse-transcribed to cDNA using a cDNA synthesis kit (Takara Bio). PCR was performed using iQ SYBR Green Supermix (Takara Bio) on a LightCycler (Roche). RNA levels were normalized to endogenous β-actin (ACTB) for each sample. Primers used are listed in Table S1.

Measurement of Ig Isotypes and Serum IL-6. Secreted IgG in the culture supernatant was quantitated by sandwich ELISA using affinity-purified goat anti-human IgG-Fc (Bethyl Laboratories). Bound IgG was measured according to the manufacturer's instructions. Serum IL-6 was measured by ELISA (R&D Systems) according to the manufacturer's instructions.

AQP4-Ab Detection Assay. Human AQP4-expressing cells were established to detect AQP4-Abs by flow cytometry. A human AQP4 (hAQP4) M23 splice variant from a clone collection (Invitrogen) was amplified by PCR and subcloned into a pIRES-DsRed-Express vector (Clontech). CHO cells (American Type Culture Collection) were transfected with this hAQP4 M23 vector (CHO^{AQP4}) or vector

Table 1. Demographic features

	HS	Seropositive patients	CMS patients
Number	20	24	17
Age	44.7 ± 2.8	47.9 ± 3.2	41.3 ± 3.0
Male:female	5:15	1:23	5:12
Disease duration		12.0 ± 1.6	9.4 ± 2.4
Age of symptom onset		36.1 ± 3.0	31.9 ± 3.4
Relapses in last 2 y		1.4 ± 0.3	0.7 ± 0.2
EDSS score in disease remission		5.0 ± 0.5	2.1 ± 0.6
Other autoantibodies		ANA 13, SS-A 5	ND

Demographic features for HS, AQP4-Ab seropositive patients, and CMS patients. Values are expressed as number or mean ± SEM. ANA, anti-nuclear antibody; ND, not detected; SS-A, anti–SS-A antibody; EDSS, expanded disability status scale.

control (CHO^{VC}) using FuGENE 6 Transfection Reagent (Roche). After 2 wk of geneticin (Invitrogen) selection, stable clones were established by single-cell sorting. The expression of hAQP4 in the established clones was confirmed using anti-human AQP4 antibody and FITC-anti-rabbit IgG antibody. Reactivity of AQP4-Abs to CHO^{AQP4} was confirmed using seropositive NMO patients' sera diluted at 1:1,000 and FITC-anti-human IgG antibody. To measure the AQP4-Ab activity in culture supernatants, these supernatants were concentrated up to 10 times using an Amicon Ultra 0.5 mL 100K device (Millipore), and 10 μL of the solution was added to 3×10^4 CHO^{AQP4} and CHO^{VC} cells. After incubation on ice for 20 min, cells were washed with sterile PBS containing 1% BSA and stained with FITC-anti-human IgG antibody. After a 10-min incubation on ice, the cells were washed and fixed for 15 min in 2% paraformaldehyde. Then the cells were washed and analyzed by flow cytometry.

Data Analysis. Histogram overlay analysis was performed using Cell Quest software (BD Biosciences). Statistics were calculated using Prism (GraphPad Software). Wilcoxon signed-rank test, Mann–Whitney *U* test, ANOVA, or Spearman's correlation test were also used when appropriate. Post hoc tests were used as a multiple comparison test after confirmation of equal variances by ANOVA.

ACKNOWLEDGMENTS. We thank T. Takahashi and K. Fujihara for establishing the diagnosis of NMO. We also thank S. Hirose for advice on morphological analysis. We also thank M. Murata, director of the Neurology Department, NCNP Hospital for kindly supporting our sample collection. This work was supported by a Health and Labour Sciences Research Grant on Intractable Diseases (Neuroimmunological Diseases) from the Ministry of Health, Labour and Welfare of Japan, and a Grant-in-Aid for Scientific Research (S) from the Japan Society for the Promotion of Science.

1. Wingerchuk DM, Lennon VA, Lucchinetti CF, Pittock SJ, Weinshenker BG (2007) The spectrum of neuromyelitis optica. *Lancet Neurol* 6:805–815.
2. Jarius S, et al. (2008) Mechanisms of disease: Aquaporin-4 antibodies in neuromyelitis optica. *Nat Clin Pract Neurol* 4:202–214.
3. Wingerchuk DM, Lennon VA, Pittock SJ, Lucchinetti CF, Weinshenker BG (2006) Revised diagnostic criteria for neuromyelitis optica. *Neurology* 66:1485–1489.
4. Tait MJ, Saadoun S, Bell BA, Papadopoulos MC (2008) Water movements in the brain: Role of aquaporins. *Trends Neurosci* 31:37–43.
5. Jarius S, et al. (2008) Antibody to aquaporin-4 in the long-term course of neuromyelitis optica. *Brain* 131:3072–3080.
6. Roemer SF, et al. (2007) Pattern-specific loss of aquaporin-4 immunoreactivity distinguishes neuromyelitis optica from multiple sclerosis. *Brain* 130:1194–1205.
7. Misu T, et al. (2007) Loss of aquaporin 4 in lesions of neuromyelitis optica: Distinction from multiple sclerosis. *Brain* 130:1224–1234.
8. Hinson SR, et al. (2009) Prediction of neuromyelitis optica attack severity by quantitation of complement-mediated injury to aquaporin-4-expressing cells. *Arch Neurol* 66:1164–1167.
9. Saadoun S, et al. (2010) Intra-cerebral injection of neuromyelitis optica immunoglobulin G and human complement produces neuromyelitis optica lesions in mice. *Brain* 133:349–361.
10. Bennett JL, et al. (2009) Intrathecal pathogenic anti-aquaporin-4 antibodies in early neuromyelitis optica. *Ann Neurol* 66:617–629.
11. Bradl M, et al. (2009) Neuromyelitis optica: Pathogenicity of patient immunoglobulin in vivo. *Ann Neurol* 66:630–643.
12. Kinoshita M, et al. (2009) Neuromyelitis optica: Passive transfer to rats by human immunoglobulin. *Biochem Biophys Res Commun* 386:623–627.
13. Kikuchi Y, et al. (2002) RP105-lacking B cells from lupus patients are responsible for the production of immunoglobulins and autoantibodies. *Arthritis Rheum* 46: 3259–3265.
14. Divanovic S, et al. (2005) Negative regulation of Toll-like receptor 4 signaling by the Toll-like receptor homolog RP105. *Nat Immunol* 6:571–578.
15. Good KL, Avery DT, Tangye SG (2009) Resting human memory B cells are intrinsically programmed for enhanced survival and responsiveness to diverse stimuli compared to naive B cells. *J Immunol* 182:890–901.
16. Wrammert J, et al. (2008) Rapid cloning of high-affinity human monoclonal antibodies against influenza virus. *Nature* 453:667–671.
17. Odendahl M, et al. (2000) Disturbed peripheral B lymphocyte homeostasis in systemic lupus erythematosus. *J Immunol* 165:5970–5979.
18. Hinson SR, et al. (2007) Pathogenic potential of IgG binding to water channel extracellular domain in neuromyelitis optica. *Neurology* 69:2221–2231.
19. Shapiro-Shelef M, et al. (2003) Blimp-1 is required for the formation of immunoglobulin secreting plasma cells and pre-plasma memory B cells. *Immunity* 19:607–620.
20. Klein U, et al. (2006) Transcription factor IRF4 controls plasma cell differentiation and class-switch recombination. *Nat Immunol* 7:773–782.
21. Kallies A, et al. (2007) Initiation of plasma-cell differentiation is independent of the transcription factor Blimp-1. *Immunity* 26:555–566.
22. Jourdan M, et al. (2009) An in vitro model of differentiation of memory B cells into plasmablasts and plasma cells including detailed phenotypic and molecular characterization. *Blood* 114:5173–5181.
23. Manz RA, Hauser AE, Hiepe F, Radbruch A (2005) Maintenance of serum antibody levels. *Annu Rev Immunol* 23:367–386.
24. Kawano MM, Mihara K, Huang N, Tsujimoto T, Kuramoto A (1995) Differentiation of early plasma cells on bone marrow stromal cells requires interleukin-6 for escaping from apoptosis. *Blood* 85:487–494.
25. Avery DT, et al. (2003) BAFF selectively enhances the survival of plasmablasts generated from human memory B cells. *J Clin Invest* 112:286–297.
26. Belnoue E, et al. (2008) APRIL is critical for plasmablast survival in the bone marrow and poorly expressed by early-life bone marrow stromal cells. *Blood* 111:2755–2764.
27. Içöz S, et al. (2010) Enhanced IL-6 production in aquaporin-4 antibody positive neuromyelitis optica patients. *Int J Neurosci* 120:71–75.
28. Yanagawa K, et al. (2009) Pathologic and immunologic profiles of a limited form of neuromyelitis optica with myelitis. *Neurology* 73:1628–1637.
29. Tsantikos E, et al. (2010) Autoimmune disease in Lyn-deficient mice is dependent on an inflammatory environment established by IL-6. *J Immunol* 184:1348–1360.
30. Ettinger R, et al. (2005) IL-21 induces differentiation of human naive and memory B cells into antibody-secreting plasma cells. *J Immunol* 175:7867–7879.
31. Iwakoshi NN, Lee AH, Glimcher LH (2003) The X-box binding protein-1 transcription factor is required for plasma cell differentiation and the unfolded protein response. *Immunol Rev* 194:29–38.
32. Linington C, Bradl M, Lassmann H, Brunner C, Vass K (1988) Augmentation of demyelination in rat acute allergic encephalomyelitis by circulating mouse monoclonal antibodies directed against a myelin/oligodendrocyte glycoprotein. *Am J Pathol* 130:443–454.
33. Takahashi T, et al. (2007) Anti-aquaporin-4 antibody is involved in the pathogenesis of NMO: A study on antibody titre. *Brain* 130:1235–1243.
34. Hoyer BF, et al. (2004) Short-lived plasmablasts and long-lived plasma cells contribute to chronic humoral autoimmunity in NZB/W mice. *J Exp Med* 199:1577–1584.
35. Okada K, Matsushita T, Kira J, Tsuji S (2010) B-cell activating factor of the TNF family is upregulated in neuromyelitis optica. *Neurology* 74:177–178.
36. Nishimoto N, et al. (2004) Treatment of rheumatoid arthritis with humanized anti-interleukin-6 receptor antibody: A multicenter, double-blind, placebo-controlled trial. *Arthritis Rheum* 50:1761–1769.
37. Nishimoto N, et al. (2005) Humanized anti-interleukin-6 receptor antibody treatment of multicentric Castleman disease. *Blood* 106:2627–2632.
38. Okamoto T, et al. (2008) Treatment of neuromyelitis optica: Current debate. *Ther Adv Neurol Disord* 1:5–12.
39. Cree BA, et al. (2005) An open label study of the effects of rituximab in neuromyelitis optica. *Neurology* 64:1270–1272.
40. Weber MS, et al. (2010) B-cell activation influences T-cell polarization and outcome of anti-CD20 B-cell depletion in central nervous system autoimmunity. *Ann Neurol* 68: 369–383.
41. Capobianco M, et al. (2007) Variable responses to rituximab treatment in neuromyelitis optica (Devic's disease). *Neurol Sci* 28:209–211.
42. Nasir S, Kerr DA, Birnbaum J (2009) Nineteen episodes of recurrent myelitis in a woman with neuromyelitis optica and systemic lupus erythematosus. *Arch Neurol* 66: 1160–1163.
43. Polman CH, et al. (2005) Diagnostic criteria for multiple sclerosis: 2005 revisions to the "McDonald Criteria." *Ann Neurol* 58:840–846.

Journal of Neuroimmunology 236 (2011) 111–117

Contents lists available at ScienceDirect

Journal of Neuroimmunology

journal homepage: www.elsevier.com/locate/jneuroim

Increase of Ki-67+ natural killer cells in multiple sclerosis patients treated with interferon-β and interferon-β combined with low-dose oral steroids

Lara Sanvito [a,b,*], Atsuko Tomita [b], Norio Chihara [b], Tomoko Okamoto [c], Youwei Lin [c], Masafumi Ogawa [c], Bruno Gran [a], Toshimasa Aranami [b], Takashi Yamamura [b]

[a] Division of Clinical Neurology, University of Nottingham, Nottingham, United Kingdom
[b] Department of Immunology, National Institute of Neuroscience, Kodaira, Tokyo, Japan
[c] Department of Neurology, National Center of Neurology and Psychiatry, Kodaira, Tokyo, Japan

ARTICLE INFO

Article history:
Received 30 October 2010
Received in revised form 26 April 2011
Accepted 11 May 2011

Keywords:
Natural killer cells
Multiple sclerosis
Interferon-β
Prednisolone
Corticosteroids

ABSTRACT

Interferon-β (IFN-β) is known to expand regulatory CD56^{bright}natural killer (NK) cells in multiple sclerosis (MS). In this cross-sectional study we show that MS patients treated with IFN-β alone or in combination with low-dose prednisolone displayed increased proportion of all NK cell subsets in the active phase of the cell cycle (Ki-67^{+}). There was no difference in NK cell apoptosis markers. In vitro experiments showed that both IFN-β and IFN-β in combination with corticosteroids increased the proportion of Ki-67^{+} NK cells. This study, although limited, shows that treatment with IFN-β affects NK cell cycle without altering NK cell apoptosis in MS patients.

1. Introduction

Interferon-β (IFN-β) has been used as mainstream treatment in multiple sclerosis (MS) for decades. Early treatment with IFN-β reduces relapse rate and disability (Goodin et al., 2002). High dose short-term intravenous steroids are commonly used to accelerate recovery from acute relapses; however, there is not enough evidence to support a protective effect on long-term disability (Ciccone et al., 2008; Myhr and Mellgren, 2009). Of note, high dose pulses of IVMP had prolonged benefit on gadolinium enhancing lesions in IFN-β treated patients as compared to patients not on treatment with IFN-β (Gasperini et al., 1998). In recent studies pulsed oral methylprednisolone (MP) as add-on therapy to subcutaneous IFN-β1a reduced relapse rate (Sorensen et al., 2009) but was not associated with reduction in long-term disability (Ravnborg et al., 2010). Combination treatment of intramuscular IFN-β1a and intravenous MP (IVMP) did not show significant benefit in relapsing-remitting MS (Cohen et al., 2009). Low-dose oral prednisolone (PDN) as add-on treatment to IFN-β is less commonly used in MS but is considered in clinical practice for patients with reduced response to IFN-β in some countries, including Japan. In a recent study IFN-β1a with either azathioprine or azathioprine with PDN in IFN-β naïve patients was not superior to monotherapy (Havrdova et al., 2009).

Natural killer (NK) cell numbers and function are thought to be altered in MS (Benczur et al., 1980; Kastrukoff et al., 2003; De Jager et al., 2008). NK cells comprise two distinct populations, CD56^{dim} with predominant cytotoxic activity and CD56^{bright} with predominant cytokine producing and possibly immunoregulatory activity (Caligiuri, 2008). To date, there are still contradicting views on the role of NK cells in the pathogenic process underlying MS (Lunemann and Munz, 2008). Reports of reduction of NK cell numbers and function in MS patients and evidence from experimental autoimmune encephalomyelitis (EAE) suggest a protective role of this population (Zhang et al., 1997; Kastrukoff et al., 2003; De Jager et al., 2008). However, this subset can also exert a detrimental role in the inflammatory process within the CNS (Winkler-Pickett et al., 2008). Interestingly, recent work in EAE suggests an organ-specific suppressive function of NK cells towards Th17 cells which are considered by someone to be the main mediators of the inflammatory process in both EAE and MS (Hao et al., 2010).

IFN-β is a type I interferon that can have opposite functional effects on different types of immune cells (Feng et al., 2002). The effects of IFN-β treatment on the adaptive and innate immune response in MS have been thoroughly investigated (Dhib-Jalbut and Marks, 2010). Treatment with IFN-β leads to a reduction of circulating total NK cells (Perini et al., 2000; Hartrich et al., 2003) and the expansion of CD56^{bright} NK cells, suggesting a protective role of this subpopulation (Saraste et al., 2007; Vandenbark et al., 2009). The mechanisms underlying the effects of IFN-β on both total and CD56^{bright} NK cells

* Corresponding author at: Division of Clinical Neurology, University of Nottingham, C Floor, South Block, Queen's Medical Centre, Nottingham NG7 2UH, United Kingdom. Tel.: +44 115 849 3363; fax: +44 115 970 9738.
E-mail address: lara.sanvito@gmail.com (L. Sanvito).

0165-5728/$ – see front matter © 2011 Elsevier B.V. All rights reserved.
doi:10.1016/j.jneuroim.2011.05.005

are still not understood. IFN-β treatment does not affect IFN-γ production and in vitro cytotoxicity of NK cells (Kastrukoff et al., 1999; Furlan et al., 2000). An expansion of $CD56^{bright}$ cells is observed after treatment with daclizumab, a monoclonal antibody against the IL-2 receptor α chain (Bielekova et al., 2006). Daclizumab leads to an IL-2 driven activation of $CD56^{bright}$ NK cells with increase in their cytotoxic activity (Martin et al., 2010). Treatment with this monoclonal antibody, either in combination with IFN-β or in monotherapy, is associated with an increased proportion of Ki-67^+ NK cells, which are considered proliferating cells (Martin et al., 2010).

In this cross-sectional study we report that in vivo treatment with IFN-β alone or in combination with low-dose PDN leads to a significant increase of NK cells in the active phase of the cell cycle (Ki-67^+). We further examined the effects of IFN-β on the ex vivo apoptotic rate of NK cells and did not find any significant difference, although IFN-β plus PDN increased the expression of the anti-apoptotic marker Bcl-2. Finally we demonstrate that in vitro treatment with IFN-β alone or in combination with corticosteroids is associated with increased proportion of Ki-67^+ NK cells.

2. Materials and methods

2.1. Subjects

Fifty-three MS patients and 15 healthy volunteers were recruited at the National Center of Neurology and Psychiatry (NCNP) in Kodaira, Tokyo, Japan. Clinical characteristic of patients and healthy subjects are summarised in Table 1a and b. Patients were classified as clinically isolated syndrome (CIS), relapsing-remitting (RR-MS), secondary progressive (SP-MS) or primary progressive (PP-MS) according to international criteria (Polman et al., 2005). Only one patient was diagnosed as pure optic-spinal form of multiple sclerosis (OS-MS), which is more common in the Japanese population (Misu et al., 2002). Patients with neuromyelitis optica were excluded. Twenty-four patients were untreated at the time of sampling (19 RR-MS, 1 CIS, 3 SP-MS, 1 PP-MS) whilst 29 patients were under treatment either with IFN-β (12 RR-MS), IFN-β + PDN (6 RR-MS) or only PDN (9 RR-MS, 1 SP-MS and 1 OS-MS). Five patients were treated with IFN-β1b (Betaferon®) and 7 patients were treated with IFN-β1a (Avonex®) in the IFN-β treated group. Three patients were treated with IFN-β1b (Betaferon®) and 3 patients were treated with IFN-β1a (Avonex®) in the IFN-β + PDN treated group. IFN-β + PDN patients were treated with low-dose steroids because of the persistence of relapses on treatment with IFN-β alone. The duration of the treatment with IFN-β alone was 2.0 (1.5) years and the duration of the treatment with IFN-β + PDN was 0.7 (0.3) years. The average (SD) daily dose of PDN was 4.6 (2.3) mg in the IFN-β + PDN group and 9.0 (4.8) mg in the PDN group. The blood was drawn at variable intervals after IFN-β injections with a range from 12 h to 6 days. All the patients were in the state of remission at the time of the study as determined by history and clinical assessment. Untreated patients had not been given any immunosuppressive medication or corticosteroids for at least 1 month before inclusion in the study.

Written informed consent was obtained from all patients and healthy volunteers and the study was approved by the Ethics Committee of the NCNP.

2.2. Isolation and stimulation of PBMC

Peripheral blood mononuclear cells (PBMC) were separated by density gradient centrifugation with Ficoll-Hypaque Plus (Amersham Biosciences, Uppsala, Sweden). To test the proportion of Ki-67^+ cells after culture in vitro, PBMC (0.5×10^6 cells per well in 200 μl final volume) were cultured for 3 days in the presence or absence of IFN-β at increasing concentrations (12.5, 25, 50, 100, 250 ng/ml; 250 ng/ml equivalent to 8,000 IU/ml) and/or dexamethasone (0.01 and 0.1 nM).

2.3. Reagents and flow cytometry

Anti CD3-PC5 and FITC, anti CD56-PE and PC5 monoclonal antibodies (mAbs) were purchased from Immunotech (Marseille, France). Anti CD3-APC, Ki-67-FITC, Bcl-2-FITC, Annexin-V-FITC mAbs and 7-AAD were purchased from BD PharMingen (San Jose, CA, USA). Interferon-β was purchased from Peprotech (Rocky Hill, NJ, USA) and dexamethasone was purchased from Sigma-Aldrich (St. Louis, MO, USA). After staining with the appropriate antibody cells were analysed on an Epics flow cytometer (Beckman Coulter, CA, USA). Stainings with anti CD3-APC, CD56-PE, Annexin-V-FITC and 7-ADD were analysed on FACS

Table 1

a. Clinical characteristics of all the subjects recruited in the study

Subjects	n	Disease type	Mean age (SD)	Sex	Mean disease duration in years (SD)	Annual relapse rate* [mean (SD)]	EDSS [median (SD)]
Healthy controls	15	–	33.5 (7.3)	6 M 9 F	–	–	–
Untreated MS	24	19 RR-MS, 1 CIS, 3 SP-MS, 1 PP-MS	43.1 (11.0)	8 M 16 F	8.3 (7.6)	1.1 (1.8)	1.3 (1.7)
IFN-β treated MS	12	12 RR-MS	29.3 (6.2)	5 M 7 F	4.6 (2.7)	1.9 (1.1)	2.3 (1.7)
IFN-β + PDN treated MS	6	6 RR-MS	40.2 (17.2)	1 M 5 F	9.3 (8.1)	1.3 (2.0)	3.3 (0.3)
PDN treated MS	11	9 RR 1 SP 1 OS	42.3 (9.6)	3 M 8 F	4.1 (3.0)	1.3 (0.8)	3.0 (1.8)

b. Clinical characteristics of treated patients recruited in the study

Subjects	n	Type T	Duration T (years)	Relapse rate BT	Relapse rate AT
IFN-β treated MS	12	IFN-β1a ($n=6$), IFN-β 1b ($n=6$)	2.0 (1.5)	1.9 (1.1)	0.1 (0.2)
IFN-β + PDN treated MS	6	IFN-β1a ($n=3$), IFN-β 1b ($n=3$)	0.7 (0.3)	1.3 (2.0)	0.1 (0.2)

*Relapse rate before starting treatment in case of IFN-β treated patients. T = treatment; BT = before treatment; AT = after treatment. IFN-β1a = Avonex®; IFN-β1b = Betaferon®.

Calibur (Becton Dickinson, NJ, USA). Weasel flow cytometry software (http://en.bio-soft.net/other/WEASEL.html) was used for data analysis.

2.4. Statistical analysis

We used Kruskall–Wallis test and Dunn's post test for 5-group comparison (healthy controls, untreated MS, IFN-β treated MS, IFN-β + PDN treated MS and PDN treated MS patients) and paired *T* test for paired samples. Correlations were performed using Spearman test. A *p* value greater than 0.05 was deemed statistically significant.

3. Results

3.1. IFN-β and (IFN-β + PDN) treated MS patients show increase of circulating Ki-67$^+$ NK cells

We found a significant increase in the proportion of Ki-67$^+$ NK cells in IFN-β and IFN-β + PDN treated patients as compared to the other groups [mean (SD): healthy controls 5.1 (2.1), untreated MS 6.2 (5.0), IFN-β treated MS 15.0 (7.9), IFN-β + PDN treated MS 29.0 (16.2), PDN treated MS patients 5.1 (2.4); $p<0.0001$, Fig. 1]. Ki-67$^+$ total NK cells were significantly increased in IFN-β treated MS patients as compared to HC ($p<0.05$), untreated MS ($p<0.01$) and PDN treated MS patients ($p<0.05$) (Fig. 1B). Similarly, Ki-67$^+$ total NK cells were significantly increased in IFN-β + PDN treated MS patients as compared to HC ($p<0.01$), untreated MS ($p<0.001$) and PDN treated MS patients ($p<0.01$). When we analysed separately CD56^{dim} and CD56^{bright} NK cells, we found that the significant increase in the proportion of Ki-67$^+$ cells was particularly evident in the CD56^{dim} subset [mean (SD): healthy controls 4.5 (2.1), untreated MS 6.1 (6.3), IFN-β treated MS 13.4 (6.8), IFN-β + PDN treated MS 29.6 (17.2), PDN treated MS patients 4.7 (2.6); $p<0.0001$]. Ki-67$^+$ CD56^{dim} NK cells were significantly increased in IFN-β treated MS patients as compared to HC ($p<0.05$), untreated MS ($p<0.01$) and PDN treated MS patients ($p<0.05$) (Fig. 1C). Similar to findings in total NK cells, Ki-67$^+$ CD56^{dim} NK cells were significantly increased in IFN-β + PDN treated MS patients as compared to HC ($p<0.01$), untreated MS ($p<0.01$) and PDN treated MS patients ($p<0.01$). Also the proportion of CD56 ^{bright} Ki-67$^+$ NK cells showed a significantly different distribution between groups ($p=0.005$). Post test analysis showed significant differences in only IFN-β + PDN treated MS patients as compared to HC ($p<0.01$) and untreated MS patients ($p<0.05$) (Fig. 1D).

Our cohort included patients with various treatment durations and we did not have longitudinal data before and after starting treatment. There were no significant differences in disease duration between groups; however, IFN-β treated patients were significantly younger than untreated MS ($p<0.01$) and PDN treated MS patients ($p<0.05$). There was a significant difference in relapse rate between groups ($p=0.03$) and in particular relapse rate was higher in IFN-β treated as compared to untreated MS patients [mean (SD) was 1.9 (1.1) versus 1.1 (1.8), respectively; ($p<0.05$)] (Table 1b). The relapse rate decreased in both IFN-β treated and IFN-β + PDN treated MS patients after treatment [mean (SD) 1.9 (1.1) before treatment and 0.1 (0.2) after treatment in IFN-β treated MS patients; 1.3 (2.0) before treatment and

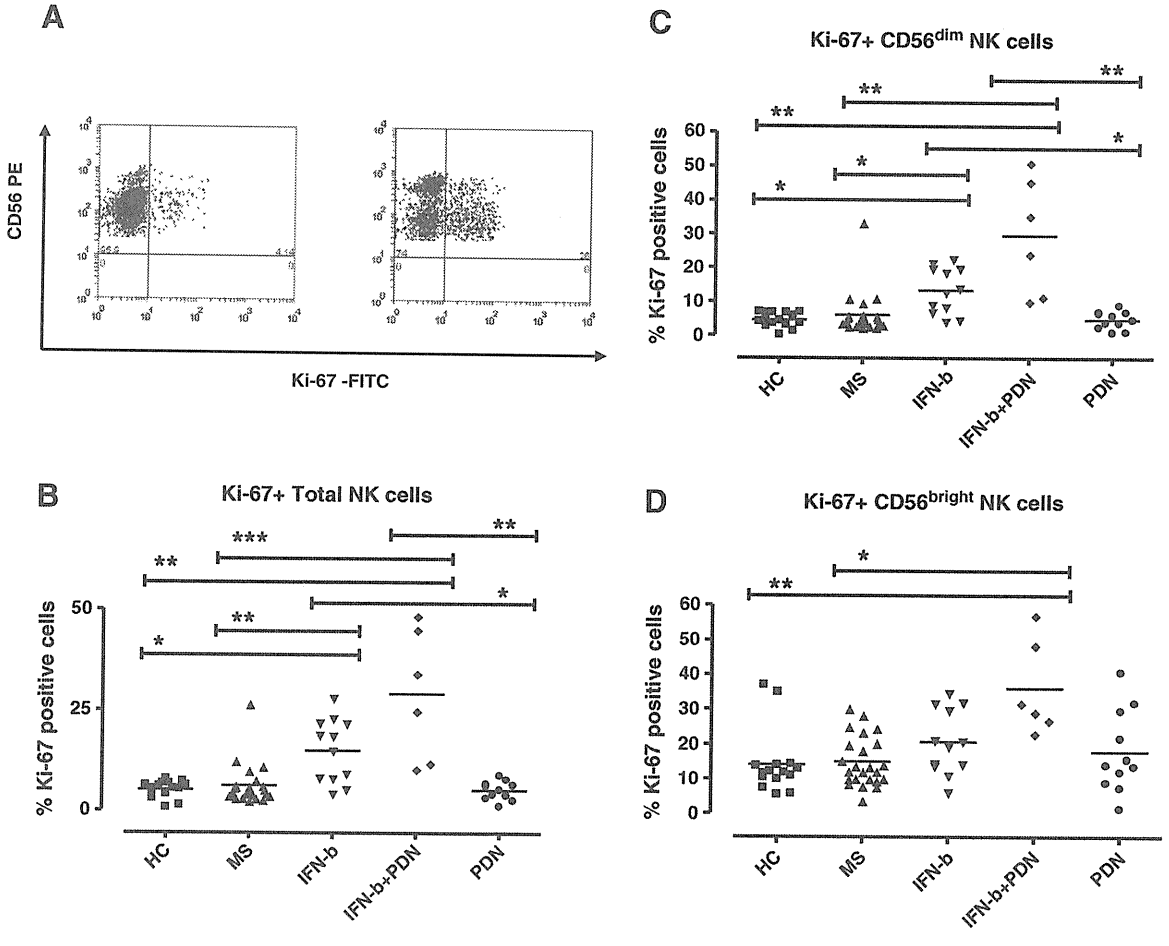

Fig. 1. Frequency of Ki-67$^+$ cells is increased in NK cells from both IFN-β treated and IFN-β + PDN treated patients. (A) Representative expression pattern of Ki-67 versus CD56 in one healthy control (left) and one IFN-β treated MS patient (right) in gated CD3$^-$ lymphocytes. (B–D) Frequency of Ki-67$^+$ total NK cells (B), CD56^{dim} NK cells (C), CD56^{bright} NK cells (D) in the five groups: healthy controls (HC), untreated MS patients (MS), IFN-β treated MS patients (IFN-b), IFN-β and prednisolone treated MS patients (IFN-b + PDN) and prednisolone only treated (PDN) treated MS patients. ***$p<0.001$, **$p<0.01$ and *$p<0.05$; Kruskall–Wallis and Dunn's post test.

0.1 (0.2) after treatment in IFN-β + PDN treated MS patients] (Table 1b). There were no correlations between the relapse rate and the proportion of circulating NK cells. There were no correlations between the percentage of Ki-67$^+$ total, CD56^{dim} or CD56^{bright} NK cells and age, relapse rate, EDSS, duration or type of treatment with IFN-β.

3.2. The number of Ki-67$^+$ NK cells correlates with reduced proportion of total and CD56^{dim} NK cells in untreated and IFN-β treated MS patients but not in normal controls

As reported previously by our group (Takahashi et al., 2001), there was no difference in the proportion of circulating CD3$^-$CD56$^+$ total NK and CD56^{dim} NK cells between untreated and treated MS patients and healthy controls (data not shown). CD56^{bright} NK cells tended to be increased in IFN-β (0.77 ± 0.71%) and IFN-β + PDN treated MS patients (1.15 ± 0.69%) as compared to HC (0.51 ± 0.25%) and untreated MS patients (0.45 ± 0.20%), but there was no significant difference comparing the four groups.

Untreated MS and IFN-β treated MS patients showed a striking inverse correlation between the proportions of total NK cells and the proportions of Ki-67$^+$ total NK cells ($p = 0.0052$ and $p = 0.028$, respectively; Fig. 2). A negative correlation was evident also between the proportions of circulating CD56^{dim} NK cells and the proportions of Ki-67$^+$ CD56^{dim} NK cells in both untreated and IFN-β treated MS patients ($p = 0.0037$ and $p = 0.005$, respectively; data not shown). There was no significant correlation in healthy controls, IFN-β + PDN and PDN treated MS patients (data not shown).

When we analysed CD56^{bright} NK cells, the negative correlation between the proportion of circulating CD56 ^{bright} NK cells and the proportion of Ki-67$^+$ CD56 ^{bright} NK cells was present in only untreated MS patients ($p = 0.034$; data not shown).

3.3. IFN-β treatment does not affect the apoptotic rate of NK cells in MS patients

To determine whether the increased Ki-67 expression of NK cells in IFN-β and IFN-β + PDN treated patients was associated with alteration of apoptotic markers, we first determined the intracellular expression of the anti-apoptotic protein Bcl-2. IFN-β treated patients showed a tendency to increased Bcl-2 expression in NK cells, although this was not statistically significant. IFN-β + PDN treated patients showed a significant increased frequency of expression of Bcl-2 in total NK, CD56^{dim} and ^{bright} NK cells as compared to MS patients ($p < 0.05$; Fig. 3A, B and C, respectively). This statistical difference was not confirmed analysing the MFI of Bcl-2 expression (data not shown).

We then examined the ex vivo proportion of apoptotic NK cell subsets by staining freshly isolated PBMC with Annexin-V and 7-AAD. Treatment with IFN-β did not alter the proportion of apoptotic (Annexin-V positive and 7-AAD negative) total NK cells as compared to untreated MS and HC (Fig. 3D). Similarly, there was no difference in the proportion of apoptotic CD56^{dim} and ^{bright} NK cells (data not shown). Unfortunately it was not possible to test IFN-β + PDN treated MS patients for Annexin-V and 7-AAD staining due to time limitations.

3.4. In vitro IFN-β increases the number of Ki-67$^+$ NK cells

To determine whether IFN-β and/or corticosteroids can directly stimulate an increase of Ki-67$^+$ NK cells, we performed in vitro experiments on PBMC freshly isolated from normal subjects. PBMC were cultured either without or with increasing high IFN-β concentrations (range: 12.5–250 ng/ml; 12.5 ng/ml equivalent to 400 IU/ml). These concentrations are above levels detected on average in MS

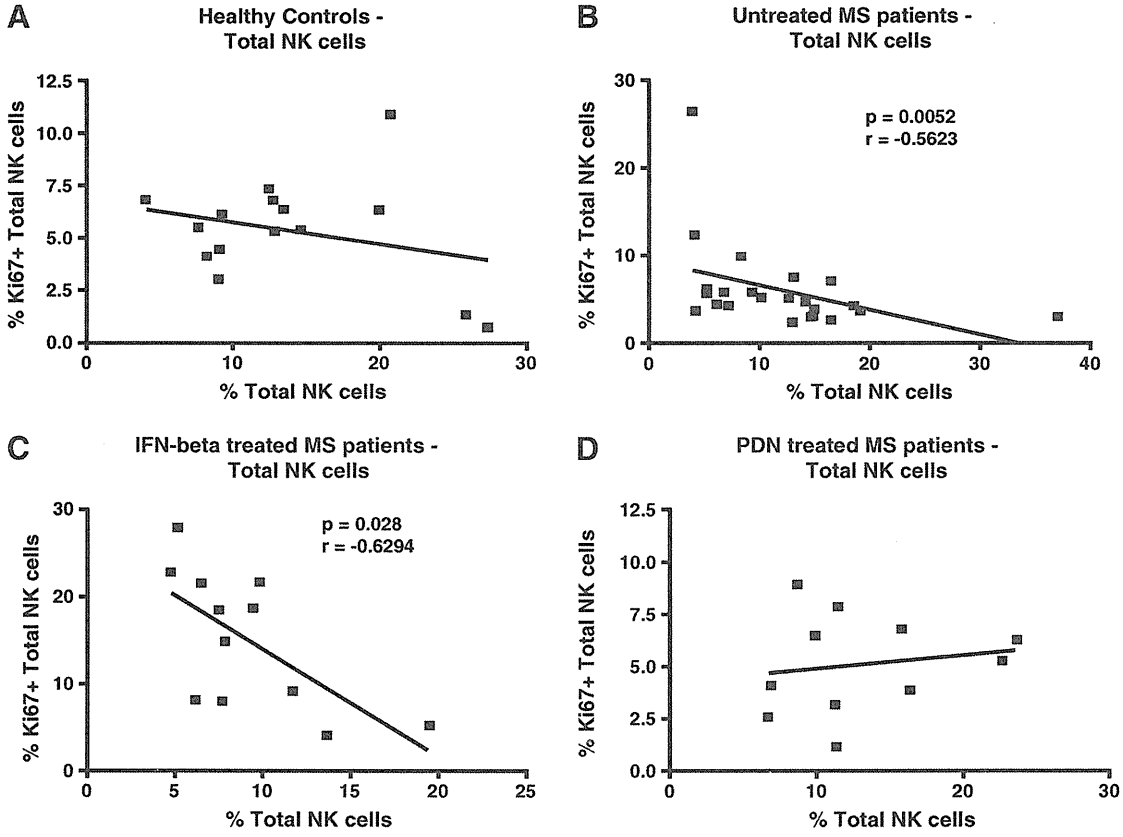

Fig. 2. The proportion of Ki-67$^+$ NK cells is inversely correlated with the proportion of circulating cells in untreated MS and IFN-β treated MS but not in HC. (A) The proportion of total NK cells and Ki-67$^+$ NK cells does not show any statistically significant correlation in either healthy controls (A) or PDN treated MS patients (D). The proportion of total NK cells and Ki-67$^+$ NK cells is inversely correlated in MS patients (B) and IFN-β treated MS patients (C). Spearman test.

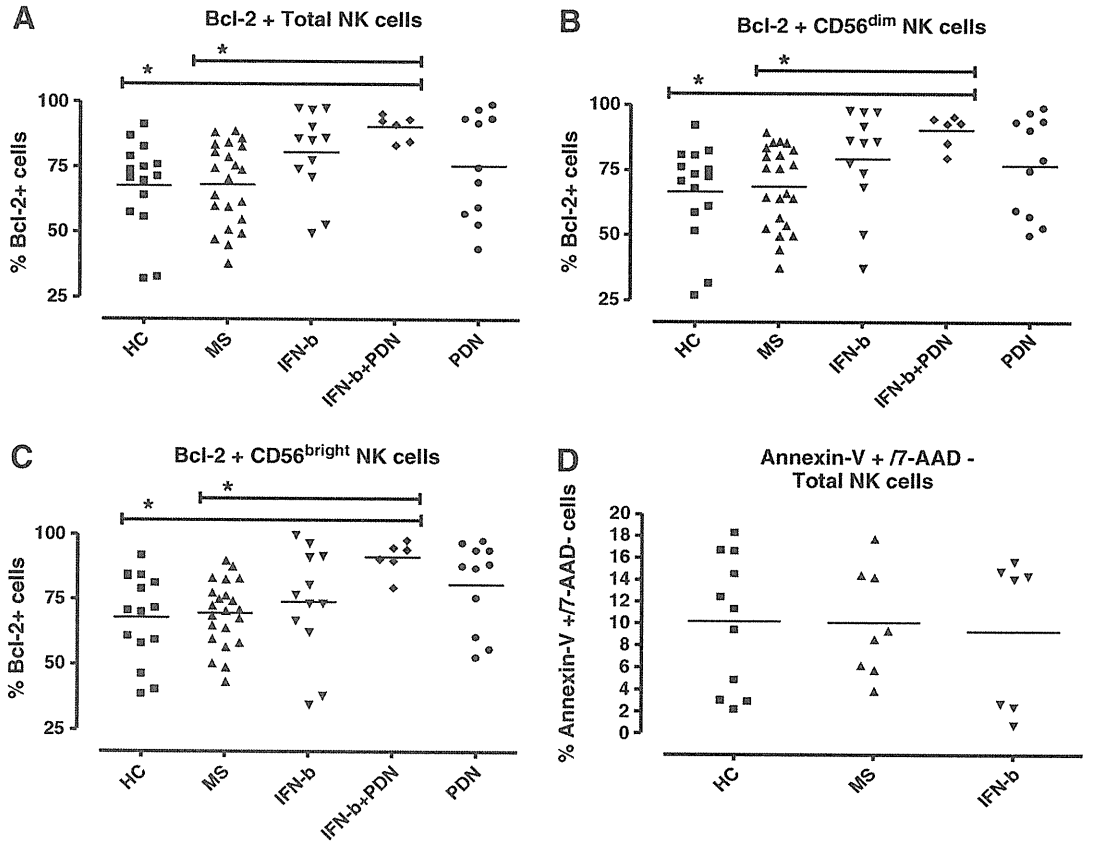

Fig. 3. Effects of IFN-β and IFN-β + PDN treatment on apoptotic markers. (A–C) The intracellular expression of Bcl-2 is significantly increased in IFN-β + PDN treated patients as compared to HC and untreated MS. (D) There was no difference in the proportion of Annexin-V$^+$/7-AAD$^-$ NK cells in HC, MS and IFN-β treated MS patients. *$p<0.05$; Kruskall–Wallis and Dunn's post test.

patients under treatment with IFN-β. Serum IFN-β levels in MS patients treated with intramuscular IFN-β1a vary between 64 and 86 IU/ml after 3 or 6 months of treatment (Khan and Dhib-Jalbut, 1998). We found that in vitro IFN-β at the highest concentration induced marked increase in NK cell apoptosis (data not shown). IFN-β significantly increased the proportion of Ki-67$^+$ NK cells at all tested concentrations but 12.5 ng/ml (Fig. 4A; $n=10$). Similar results were found with purified NK cells (data not shown). We then examined the in vitro effect of IFN-β + dexamethasone (DEX) (Fig. 4B; $n=4$). Cells were cultured either without or with 25 ng/ml of IFN-β and/or DEX (0.01 or 0.1 nM, equivalent to 3.925 and 39.25 pg/ml, respectively). We found a significant increase of Ki-67$^+$ NK cells in IFN-β + DEX culture at the concentration of 0.1nM of DEX ($p=0.046$) and a trend at the lower concentration of 0.01 nM ($p=0.07$) as compared to medium. There was no difference after culture with only DEX at either 0.1 or 0.01 nM concentration.

4. Discussion

Here we show that treatment with IFN-β and IFN-β + PDN in MS patients leads to expansion of NK cells in the active phase of the cell cycle (Ki-67$^+$). This expansion was most evident in CD56^{dim} NK cells. We also show that treatment with IFN-β does not significantly affect the apoptotic rate of NK cells. Of note, our patients were treated with either IFN-β or IFN-β combined with low-dose oral steroids and did not receive regular high dose pulses of steroids. In vitro experiments showed that IFN-β either alone or in combination with corticosteroids can increase the proportion of Ki-67$^+$ NK cells, suggesting a direct effect of IFN-β on NK cells.

IFN-β leads to reduction of circulating total NK cells and expansion of CD56^{bright} NK cells in MS patients (Perini et al., 2000; Hartrich et al., 2003; Saraste et al., 2007; Vandenbark et al., 2009). Moreover, it increases activated (CD69$^+$) NK cells but does not affect NK function (Kastrukoff et al., 1999; Furlan et al., 2000; Hartrich et al., 2003). Of note, the in vivo effects observed in MS patients do not necessarily correspond to the in vitro effects of IFN-β on NK cells. IFN-β in vitro inhibits IL-2 induced proliferation of NK cells and increases their IFN-β production (Hunter et al., 1997). To date, the mechanisms underlying the effects of IFN-β treatment on NK cell populations in MS are not completely understood. Two potential mechanisms can be hypothesised to explain the reduction of circulating NK cells associated with IFN-β treatment: (1) increase in turnover and apoptosis of either activated or resting NK cells; (2) redistribution of NK cells with migration to the peripheral tissues and particularly the CNS. These mechanisms could target either total NK cells or selectively CD56^{dim} and CD56^{bright} subsets. A gradual change in total NK numbers during treatment with IFN-β has been observed in MS patients, suggesting a gradual shift in immune homeostasis (Perini et al., 2000; Hartrich et al., 2003). Maximal reduction in NK cell numbers occurs 8 h after administration with persistent reduction at 3 months and return to baseline levels at 6 months (Hartrich et al., 2003).

Our study showed that IFN-β is associated with increased frequency of Ki-67$^+$ NK cells in a cross-sectional cohort of MS patients. Ki-67 is a nuclear antigen that is expressed exclusively in the active stages of the cell cycle, namely, late G1, S, G2 and M phases (Gerdes et al., 1984). The expression of Ki-67 starts at the first S phase, is present in mitosis and decreases in G1 (Lopez et al., 1991). The increased expression of Ki-67 in NK cells may reflect increased in vivo proliferation or accumulation of NK cells in one specific phase of the cell cycle but G0.

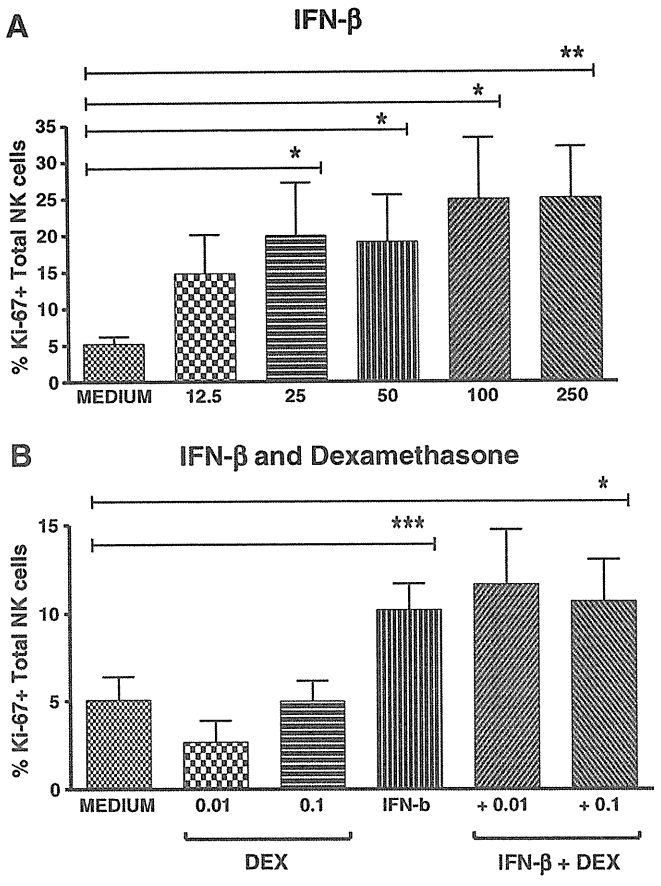

Fig. 4. In vitro effects of IFN-β and IFN-β + dexamethasone (DEX) on Ki-67$^+$ NK cells. PBMC were isolated from normal subjects and cultured for 3 days in medium without or with IFN-β and/or DEX at different concentrations. (A) IFN-β significantly increased the proportion of Ki-67$^+$ NK cells ($n=10$) as compared to medium (12.5 ng/ml, $p=0.06$; 25 ng/ml, $p=0.05$; 50 ng/ml, $p=0.04$; 100 ng/ml, $p=0.03$; 250 ng/ml, $p=0.01$). (B) Cells were cultured either without or with 25 ng/ml of IFN-β and/or DEX (0.01 or 0.1 nM respectively). IFN-β + DEX significantly increased the proportion of Ki-67$^+$ NK cells at the concentration of 0.1 nM and showed a trend at the concentration of 0.01 nM ($n=4$; $p<0.05$ and $p=0.07$, respectively). In this set of experiments IFN-β but not DEX alone significantly increased the proportion of Ki-67$^+$ NK cells as compared to medium ($p\leq0.001$). $^*p\leq0.05$, $^{**}p\leq0.01$, $^{***}p\leq0.001$; paired *T* test.

Our study showed that CD56^{dim} NK cells as well as the CD56^{bright} subset are affected by IFN-β treatment. Indeed, the increase in Ki-67$^+$ NK cells was mostly evident in the CD56^{dim} subsets. CD56^{bright} are considered precursors of CD56^{dim} NK cells (Caligiuri, 2008). The two subsets exert distinct functions and may have different roles in regulating the immune response in the periphery and/or in the CNS. The increase of Ki-67$^+$ total NK cells may therefore reflect the expansion of CD56^{bright} subset that has matured into CD56^{dim}. It is still not clear whether the expansion of CD56^{bright} cells in IFN-β treated patients reflects the correction of an underlying defect of NK cell homeostasis in MS patients or whether it is only a physiological effect of IFN-β on NK cells. Moreover, it is not known whether the expansion of CD56^{bright} NK cells is associated with clinical response to IFN-β treatment and can be considered a marker of its therapeutic effect. We did not find any correlation between the proportion of Ki-67$^+$ NK cells and clinical parameters in our study.

This is the first study to examine the effects of combined treatment with IFN-β and corticosteroids on NK cells. Our in vivo observations suggest an increased proportion of Ki-67$^+$ NK cells in IFN-β + PDN treated patients as compared to IFN-β alone but there were no statistically significant differences between the two groups. Similarly, our in vitro observations did not support a prominent effect of corticosteroids over IFN-β in increasing the proportion of Ki-67$^+$ NK cells.

NK cell homeostasis is maintained through the balance between proliferation and cellular loss. We did not find an increased rate of NK apoptosis in IFN-β treated MS patients. IFN-β induced apoptosis of unfractionated peripheral blood lymphocytes (PBLs) in MS patients (Gniadek et al., 2003). However IFN-β treated MS patients showed reduction and normalisation of ex vivo T cell apoptosis (Garcia-Merino et al., 2009). It is likely that in vivo IFN-β treatment exerts different effects on the apoptosis of different cell populations. We observed an increased expression of the anti-apoptotic molecule Bcl-2 in IFN-β + PDN treated patients, suggesting a possible synergistic effect of IFN-β and steroids in preventing NK cell apoptosis. Corticosteroids usually induce apoptosis of immune cells (Wyllie, 1980). However, high dose methylprednisolone (MP) induced unfractionated PBL and T cell apoptosis but did not have any effect on the rate of apoptotic NK cells in MS patients (Leussink et al., 2001). Of note, the observed increased Bcl-2 expression does not necessarily correlate with reduced ex vivo apoptosis of NK cells and could represent the effect of changes in the cytokine milieu secondary to the combined treatment of IFN-β + PDN (Graninger et al., 2000).

We found that the proportion of Ki-67$^+$ NK cells was inversely correlated with the proportion of circulating NK cells in both untreated and IFN-β treated MS patients. This is consistent with an inverse correlation between NK cell numbers and expression of NK activation markers (CD69$^+$ NK cells) (Hartrich et al., 2003). NK cell activation requires migration into the tissues and results in reduced NK frequency in the periphery. We hypothesise that IFN-β treatment may be associated with increased migration of activated and proliferating NK cells to the periphery and/or the CNS. Since the inverse correlation between NK cell proportion and Ki-67$^+$ NK cells was also observed in untreated MS patients, this phenomenon may represent an attempt of the immune system to regulate the inflammatory process. In this instance, IFN-β treatment would enhance a protective mechanism that occurs also in untreated MS patients in remission.

In conclusion, here we demonstrate that treatment with IFN-β in either monotherapy or combination with corticosteroids increases the proportion of NK cells in the active phase of the cell cycle both in vivo and in vitro. We hypothesise that increased proliferation and migration of NK cells to the peripheral tissues may be involved in the disease-modifying effects of IFN-β in MS patients.

Acknowledgements

This work was supported by grants from Grant-in-Aid for Scientific Research (S) from the Ministry of Education, Culture, Science and Technology (Japan) and an International Joint Project Grant from The Royal Society (United Kingdom). We thank Ms Hiromi Yamaguchi for technical assistance.

References

Benczur, M., Petrányl, G.G., Pálffy, G., Varga, M., Tálas, M., Kotsy, B., Földes, I., Hollán, S.R., 1980. Dysfunction of natural killer cells in multiple sclerosis: a possible pathogenetic factor. Clin. Exp. Immunol. 39 (3), 657–662.

Bielekova, B., Catalfamo, M., Reichert-Scrivner, S., Packer, A., Cerna, M., Waldmann, T.A., McFarland, H., Henkart, P.A., Martin, R., 2006. Regulatory CD56(bright) natural killer cells mediate immunomodulatory effects of IL-2Ralpha-targeted therapy (daclizumab) in multiple sclerosis. Proc. Natl Acad. Sci. USA 103, 5941–5946.

Caligiuri, M.A., 2008. Human natural killer cells. Blood 112, 461–469.

Ciccone, A., Beretta, S., Brusaferri, F., Galea, I., Protti, A., Spreafico, C., 2008. Corticosteroids for the long-term treatment in multiple sclerosis. Cochrane Database Syst Rev, CD006264.

Cohen, J.A., Imrey, P.B., Calabresi, P.A., Edwards, K.R., Eickenhorst, T., Felton 3rd, W.L., Fisher, E., Fox, R.J., Goodman, A.D., Hara-Cleaver, C., Hutton, G.J., Mandell, B.F., Scott, T.F., Zhang, H., Apperson-Hansen, C., Beck, G.J., Houghtaling, P.L., Karafa, M.T., Stadtler, M., 2009. Results of the Avonex Combination Trial (ACT) in relapsing-remitting MS. Neurology 72, 535–541.